

# Influence of Temperature Change on Modal Analysis of Rotary Functionally Graded Nano-beam in Thermal Environment

E. Shahabinejad, N. Shafiei, M. Ghadiri \*

*Faculty of Engineering, Department of Mechanics, Imam Khomeini International University, Qazvin, Iran*

Received 17 July 2018; accepted 20 September 2018

## ABSTRACT

The free vibration analysis of rotating functionally graded (FG) nano-beams under an in-plane thermal loading is provided for the first time in this paper. The formulation used is based on Euler-Bernoulli beam theory through Hamilton's principle and the small scale effect has been formulated using the Eringen elasticity theory. Then, they are solved by a generalized differential quadrature method (GDQM). It is supposed that, according to the power-law form (P-FGM), the thermal distribution is non-linear and material properties are dependent to temperature and are changing continuously through the thickness. Free vibration frequencies are obtained for two types of boundary conditions; cantilever and propped cantilever. The novelty of this work is related to vibration analysis of rotating FG nano-beam under different distributions of temperature with different boundary conditions using nonlocal Euler-Bernoulli beam theory. Presented theoretical results are validated by comparing the obtained results with literature. Numerical results are presented in both cantilever and propped cantilever nano-beams and the influences of the thermal, nonlocal small-scale, angular velocity, hub radius, FG index and higher modes number on the natural frequencies of the FG nano-beams are investigated in detail.

© 2018 IAU, Arak Branch. All rights reserved

**Keywords :** Rotating Euler-Bernoulli beam, FG Nano-beam, Eringen elasticity theory, GDQM, Thermal vibration.

## 1 INTRODUCTION

**N**ANOTECHNOLOGY has productive capabilities; new tools and systems with superior properties in small scale (1-0.01nm). In the past decade this multidisciplinary field has been assigned as especial filed of research in engineering sciences and technology, especially in medical applications: new nano-structural drugs, nano-robotics, drug delivery to the designated location in body and genetic defect elimination (Bath and Turberfield [2], Chen et al., [5], Goel and Vogel [15], Lee et al., [17], Lubbe et al., [19], Tierney et al., [30], Van Delden et al.,[32]). Advancing of material technology in recent decades, functionally graded materials have been widely entered in nano industry. FGMs are composite materials with heterogeneous microstructure. Their mechanical properties continuously change from one interface to another. A common combination type is the aggregation of ceramic and metal. Due to the materials composition, their mechanical properties change continuously through thickness. This

\*Corresponding author. Tel.: +98 28 33901144 ; Fax: +98 28 33780084.  
E-mail address: [ghadiri@eng.ikiu.ac.ir](mailto:ghadiri@eng.ikiu.ac.ir) (M.Ghadiri).

type of materials are widely used in industries such as: aerospace, mechanical, nuclear, electrical, shipbuilding, medical and optical applications. Among the different nano-structures, nano-beams have important applications (Hu et al., [16]). Since investigating nano-beams behaviors through experimental tests are difficult and expensive; the continuum mechanics theory is a suitable method for studying the mechanical behavior of nano-beams such as free and forced vibration, bending, buckling and etc. The classical continuum theories are unable to predict the behavior of small-scale mechanics. But researchers are able to solve this problem by providing improved theories like, nonlocal elasticity theory of Eringen [9], Strain gradient (Mindlin [21]) and coupled stress (Toupin[31]). The nonlocal elasticity theory of Eringen [9] is a common tool for analyzing structures with small scale. In this theory, unlike the classical theory, the stress at a reference point( $x$ ) in a body depends not only on the strain of that point but also of all points of the body. Based on this theory, many studies have been conducted to investigate the behavior of nano-beams. Thai [29] used this theory for bending, buckling, and free linear vibration analysis of nano-beams. Rahmani and Pedram [25] showed the analysis and modeling of vibrating nano-beams based on Timoshenko beam theory. (Ghorbanpour-Arani et al., [14]) presented the analysis of free and forced vibrations of double viscoelastic piezoelectric nano-beam systems incorporating nonlocal viscoelasticity theory and Euler–Bernoulli beam model. (Maraghi et al., [20]) based on nonlocal piezo-elasticity theory and Euler–Bernoulli beam model, investigated the nonlinear vibration and instability of embedded DWBNNT conveying viscose fluid. Furthermore, many great studies have been done on vibration analysis of rotating nano-beams. Narendar[23] studied the free flap wise bending vibration of rotating nanotube. Developing a single nonlocal beam model and employing it to study the flap wise bending vibration characteristics of a rotating nano-cantilever were done by Pradhan and Murmu [24]. Aranda-Ruiz et al. [1] calculated the non-dimensional frequencies of the flap wise bending vibrations of a non-uniform rotating nano-cantilever and considered the nonlocal boundary conditions variation by time. Also recently, Ghadiri and Shafiei [10-11] investigated linear and nonlinear bending vibration of a rotating nano-beam for various boundary conditions based on nonlocal Eringen's theory. Also, in the other research they presented the influence of surface effect on vibration behavior of rotary FG nano-beam (Ghadiri et al., [13]).

As it was noted above, a common type of FGMs are the continuous combined of ceramics and metals. FGMs can be used as a thermal barriers, thermal coatings and corrosion resistant coatings. Nowadays, as the ceramics provide the high-temperature resistance due to their low thermal conductivity, these new materials are widely used in high temperature environments. For structures working in environments with high temperatures, using FGM coating can help to effectively reduce the possible failures induced by thermo or combined thermo-mechanical loadings. The essential using of these materials in high temperature environments needs to consider the thermal effects on static and dynamic behavior of Functionally Graded Material. (Ebrahimi and Barati [7]) investigated thermal stresses in curved Functionally Graded nano-beams based on nonlocal strain gradient theory. (Mirjavadi et al., [22]) examined the buckling and free vibration of axially FG nano-beams in different thermal environment. DQ method is a new numerical technique for solving ordinary or partial equations of different boundary condition. As an alternative method of more efficiency, with acceptable accuracy and using less grid points, Bellman et al. introduced DQM in the early 1970s (Bellman and Casti [3], Bellman et al., [4]). DQM's accuracy is affected by the accuracy of weight coefficients which is influenced by the choice of grid points. In the preliminary formulations of DQM, weight coefficients were calculated by an algebraic equation system which limited the use of large grid numbers. Shu [26] presented simple explicit formula for the weight coefficients with practically unlimited number of grid points leading to GDQM. Early applications of GDQ were limited to regular domain problems. Shu and Richards [27] developed a domain decomposition technique for the study of multi-domain problems. According to this method, the domain of the problem is divided into a number of sub-domains or elements before discretizing each subdomain using GDQ. Domain decomposition technique with the use of GDQ method on each sub-domain is frequently named as the differential quadrature element method (DQEM) (Shu [26]). Recently a method called weak form quadrature element method was introduced by coupling GDQ with the weak form solution of differential equations, so that derivatives of field variables are calculated with GDQ method (Xing and Liu [34], Zhong and Yue [35]).

In the previous researches, the lack of a linear model has been sensed for comprehensive inspection of FG-rotating nano-beams free vibration with respect to thermal effects. In most of the previous studies, no literature is available for rotating nano-structures using FGM. So, there is a serious necessity to understand the vibration behavior of rotating nano-beams in FG structure with considering the effect of temperature changes. In the present paper, the vibration analysis of FG rotating nano-beam is performed with considering the effects of non-linear and size-dependent effects based on nonlocal elasticity of Eringen theory. It is assumed that material properties of the beam, vary continuously through the beam thickness according to power-law relation. Nonlocal Euler-Bernoulli beam model and Eringen's nonlocal elasticity theory are utilized. Governing equation is derived by Hamiltonian principle. Boundary conditions are cantilever and propped cantilever. These equations are solved using GDQ

method. The accuracy and reliability of this model is verified by comparing the analytical solutions and the results from the existing published work. A good agreement is observed between the results of this article and those published work. After validating the presented formulation, the variation of the first three modes non-dimensional frequencies for cantilever and propped cantilever FG nano-beams under the effects of different parameters such as nonlocal parameter, gradient index, non-dimensional angular velocity, hub radius and temperature change are investigated. This paper could be served as benchmarks for the design of nano-electronic, nano-drive devices, nano-turbine, molecular rotors and motors, nano-sensors, medical applications such as drug delivery to cancer cells, nano-robotics, tissue engineering and nano-structure drugs in which nano-beams act as basic elements. They can also be applicable as important sources for validating other approaches and approximations.

## 2 MATHEMATICAL FORMULATION

A FG nano-beam with the length dimensions of  $L$ , width  $b$  and thickness  $h$  is shown in Fig 1. It is made by composing of two different materials (pure ceramic top and pure metal down). The material properties of the beam (such as Young's Modulus  $E$ ) are assumed to vary continuously through the beam thickness. According to low power form (Ghadiri et al.,[13]):

$$P(z, T) = (P_U - P_L) \left( \frac{z}{h} + \frac{1}{2} \right)^n + P_L \quad (1)$$

According the Eq.(1), Young's Modulus and density terms can be expressed as follows:

$$E(z, T) = (E_U - E_L) \left( \frac{z}{h} + \frac{1}{2} \right)^n + E_L \quad (2)$$

$$\rho(z, T) = (\rho_U - \rho_L) \left( \frac{z}{h} + \frac{1}{2} \right)^n + \rho_L \quad (3)$$

where  $P_U$  and  $P_L$  are the material properties at the upper (ceramic) and lower (metal) surfaces and  $n$  is a non-negative number that expresses the material variation profile through the thickness of the beam. Due to dependency of material properties to temperature, it is necessary to consider the following nonlinear equation of material thermo-elastic properties to predict the behavior of functionally graded nano-beams according to the temperature. So this equation can be written as (Ebrahimi and Salari [8]):

$$n = n_0 (n_{-1} T^{-1} + 1 + n_1 T + n_2 T^2 + n_3 T^3) \quad (4)$$

where  $n_0, n_{-1}, n_1, n_2$  and  $n_3$  are the temperature dependent coefficients for  $Si_3N_4$  at the top surface (pure ceramics) and  $SUS304$  at the bottom one (pure metal). These material properties are shown in Table 1.

**Table 1**

Temperature dependent coefficients of Young's modulus, thermal expansion coefficient, mass density and Poisson's ratio for  $Si_3N_4$  and  $SUS304$ .

Material	Properties	$n_0$	$n_{-1}$	$n_1$	$n_2$	$n_3$
$Si_3N_4$	$E(Pa)$	348.43e+9	0	-3.070e-4	2.160e-7	-8.946e-11
	$\alpha(K^{-1})$	5.8723e-6	0	9.095e-4	0	0
	$\rho(Kg / m^3)$	2370	0	0	0	0
	$\nu$	0.24	0	0	0	0
$SUS304$	$E(Pa)$	201.04e+9	0	3.079e-4	-6.534e-7	0
	$\alpha(K^{-1})$	12.330e-6	0	8.086e-4	0	0
	$\rho(Kg / m^3)$	8166	0	0	0	0
	$\nu$	0.3262	0	-2.002e-4	3.797e-7	0

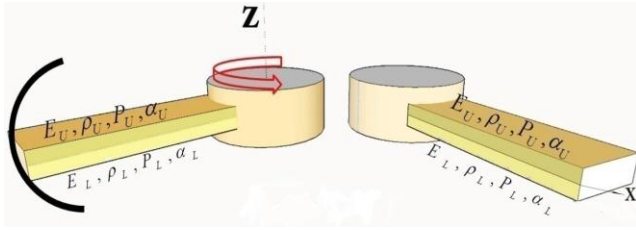


**Fig. 1** Schematic of rotating nano-beams; left figure: propped cantilever nano-beam, right figure: cantilever nano-beam.

Based on the Euler-Bernoulli theory, displacement of any point of the beam is given by (Ghadiri et al., [13]):

$$U(x, z, t) = u_0(x, t) - z \frac{\partial w(x, t)}{\partial x} \tag{5a}$$

$$W(x, z, t) = w(x, t) \tag{5b}$$

where  $U, W$  are axial displacement, and transverse displacement and  $u_0, w$  are their calculated counterparts at the mid-plane. According to the Euler-Bernoulli beam theory, the nonzero strain can be written as follows:

$$\epsilon_{xx} = \frac{\partial u_0(x, t)}{\partial x} - z \frac{\partial^2 w(x, t)}{\partial x^2} = \epsilon_{xx}^0 - zk^0 \tag{6}$$

where  $\epsilon_{xx}^0, k^0$  are extensional strain and bending strain. For the motion equation, the Hamilton's principle states that (Tauchert [28]):

$$\int_{t_2}^{t_1} (\delta U + \delta V - \delta T) dt = 0 \tag{7}$$

where the strain energy  $\delta U$ , the potential of external loading  $\delta V$  and the kinetic energy  $\delta T$  are:

$$\delta U = b \int \int_{-\frac{h}{2}}^{\frac{h}{2}} \sigma_{xx}(z) \delta \epsilon_{xx} dz dx = b \int \int_{-\frac{h}{2}}^{\frac{h}{2}} \sigma_{xx}(z) (\delta \epsilon_{xx}^0 - z \delta k^0) dz dx = b \int (N \delta \epsilon_{xx}^0 - M \delta k^0) dx, \tag{8a}$$

$$\delta V = -b \int \left[ f \delta u_0 + q \delta w + \bar{N} \frac{\partial w}{\partial x} \frac{\partial \delta w}{\partial x} \right] dx, \tag{8b}$$

$$\delta T = b \int \int_{-\frac{h}{2}}^{\frac{h}{2}} \rho(z) \left[ \left( \frac{\partial u_0}{\partial t} - z \frac{\partial^2 w}{\partial t \partial x} \right) \left( \frac{\partial \delta u_0}{\partial t} - z \frac{\partial^2 \delta w}{\partial t \partial x} \right) + \frac{\partial w}{\partial t} \frac{\partial \delta w}{\partial t} \right] dz dx = \tag{8c}$$

$$b \int \left[ I_0 \left( \frac{\partial u_0}{\partial t} \frac{\partial \delta u_0}{\partial t} + \frac{\partial w}{\partial x} \frac{\partial \delta w}{\partial x} \right) - I_1 \left( \frac{\partial u_0}{\partial t} \frac{\partial^2 \delta w}{\partial t \partial x} + \frac{\partial^2 w}{\partial t \partial x} \frac{\partial \delta u_0}{\partial t} \right) + I_2 \frac{\partial^2 w_0}{\partial t \partial x} \frac{\partial^2 \delta w}{\partial t \partial x} \right] dx,$$

where  $b, N, M$  and  $I$  are the beam width, force and moment resultant and mass moment of inertias, respectively.

$$N = \int_{-\frac{h}{2}}^{\frac{h}{2}} \sigma_{xx}(z) dz, \tag{9a}$$

$$M = \int_{-\frac{h}{2}}^{\frac{h}{2}} z \sigma_{xx}(z) dz, \tag{9b}$$

$$\begin{cases} I_0 \\ I_1 \\ I_2 \end{cases} = \int_{-\frac{h}{2}}^{\frac{h}{2}} \begin{cases} 1 \\ z \\ z^2 \end{cases} \rho(z) dz, \quad (9c)$$

By substituting Eq. (8) into Eq. (7), Euler-Lagrange equation is obtained as:

$$\frac{\partial N}{\partial x} + f = I_0 \frac{\partial^2 u_0}{\partial t^2} - I_1 \frac{\partial^3 w}{\partial t^2 \partial x} \quad (10a)$$

$$\frac{\partial^2 M}{\partial x^2} + q - \frac{\partial}{\partial x} \left( \bar{N} \frac{\partial w}{\partial x} \right) = I_0 \frac{\partial^2 w}{\partial t^2} + I_1 \frac{\partial^3 u_0}{\partial t^2 \partial x} - I_2 \frac{\partial^4 w}{\partial t^2 \partial x^2} \quad (10b)$$

$f(x,t)$ ,  $q(x,t)$  are the axial and transverse distributed forces and  $\bar{N}$  is applied for axial compressive force and it can be written as (Ghadiri et al., [12]):

$$\bar{N} = \int_{-\frac{h}{2}}^{\frac{h}{2}} [E(z)\alpha(z)(T - T_0) + N^r] dA \quad (11)$$

where:

$$\alpha(z, T) = (\alpha_U - \alpha_L) \left( \frac{z}{h} + \frac{1}{2} \right)^n + \alpha_L \quad (12)$$

where  $\alpha(z)$  is thermal expansion coefficient  $\alpha_U$  and  $\alpha_L$  are relating to ceramic phase (top of surface) and metal phase (at bottom surface), respectively. For considering the rotation of the beam, rotating terms  $N^r(x)$  can be expressed as Eq.(13) (Aranda-Ruiz et al., [1], Pradhan and Murmu [24]).

$$N^r(x) = b \int_{x-h/2}^L \int_{-h/2}^{h/2} \frac{\rho(z)\Omega^2}{2} (r + \zeta) dz d\zeta \quad (13)$$

where  $T(z)$  is considered to distribute non-linearly across its thickness. So, the beam initial temperature is assumed to be  $T_0$  and the temperature of the top surface of FG nano-beam (ceramic-rich) is  $T_U$  and it is considered to vary non-linearly along the thickness from  $T_U$  to the bottom surface (Metal-rich) temperature  $T_L$ . Therefore, in this case, the temperature distribution through the thickness has been given according to the following approach (Ebrahimi and Salari [8]).

$$T = T_L + \Delta T \left( \frac{1}{2} + \frac{z}{h} \right)^\alpha \quad (14)$$

where  $\Delta T = T_U - T_L$  and  $\alpha$  is the temperature index and  $0 < \alpha < \infty$ . The linear rise of the temperature is obtained as a particular case by setting  $\alpha = 1$ . It should be noted that, with increasing the temperature, the material behavior also changes and this behavior is important in high temperatures especially in FGMs. So, it is necessary to consider that the temperature dependent material properties. In this paper, it is assumed that  $\alpha = 0.5$ . For free vibration analysis the, Eq. (10), are reduced to

$$\frac{\partial N}{\partial x} = I_0 \frac{\partial^2 u_0}{\partial t^2} - I_1 \frac{\partial^3 w}{\partial t^2 \partial x} \quad (15a)$$

$$\frac{\partial^2 M}{\partial x^2} - \frac{\partial}{\partial x} \left( \bar{N} \frac{\partial w}{\partial x} \right) = I_0 \frac{\partial^2 w}{\partial t^2} + I_1 \frac{\partial^3 u_0}{\partial t^2 \partial x} - I_2 \frac{\partial^4 w}{\partial t^2 \partial x^2} \quad (15b)$$

2.1 Nonlocal theory

$$\sigma_{ij} = \int_v \alpha(|x' - x|, \tau) [C_{ijkl} \varepsilon_{kl}] dx' \tag{16}$$

This equation shows that the stress at point  $x$  in a body depends on strain at that point and the adjacent point. where  $\sigma_{ij}, \varepsilon_{kl}, C_{ijkl}$  are stress, strain, and elasticity Modulus tensors, respectively.  $\alpha(|x'-x|)$  is a nonlocal kernel and  $\tau=e_0a/l$  is a material constant that is explained as a small scale factor, where  $e_0$  is a material constant which is determined experimentally or by other ways.  $a$  and  $l$  are internal (e.g. lattice parameter) and external characteristic lengths (e.g. crack length, wave length) of the nano-beam, respectively. Due to the spatial integrals in the constitutive Eq. (16), it is difficult to obtain the solution of nonlocal stress problems but, according to Eringen [9] we can convert this equation to the equivalent differential constitutive equation form

$$(1 - (e_0a)^2 \nabla^2) \sigma = c : \varepsilon \tag{17}$$

For an Euler-Bernoulli nonlocal functionally graded beam, the Eq.(17) can be written as:

$$\sigma_{xx} - (e_0a)^2 \frac{\partial^2 \sigma_{xx}}{\partial x^2} = E(z) \varepsilon_{xx} \tag{18}$$

Integrating Eq. (18) over the beam's cross-section area, the axial force-strain relation can be written as:

$$N - (e_0a)^2 \frac{\partial^2 N}{\partial x^2} = b \left[ \int_{-\frac{h}{2}}^{\frac{h}{2}} E(z) dz \right] \varepsilon_{xx}^0 - b \left[ \int_{-\frac{h}{2}}^{\frac{h}{2}} z E(z) dz \right] k^0 \tag{19}$$

By multiplying Eq. (18) by  $z$ , integrating over the cross-section area, the moment–curvature relation can be written as:

$$M - (e_0a)^2 \frac{\partial^2 M}{\partial x^2} = b \left[ \int_{-\frac{h}{2}}^{\frac{h}{2}} z E(z) dz \right] \varepsilon_{xx}^0 - b \left[ \int_{-\frac{h}{2}}^{\frac{h}{2}} z^2 E(z) dz \right] k^0 \tag{20}$$

Differentiating Eq. (15a) once with respect to  $x$  and substituting it into Eq. (18)

$$N = b \left[ \int_{-\frac{h}{2}}^{\frac{h}{2}} E(z) dz \right] \frac{\partial u_0}{\partial x} - b \left[ \int_{-\frac{h}{2}}^{\frac{h}{2}} z E(z) dz \right] \frac{\partial^2 w}{\partial x^2} + (e_0a)^2 \left[ I_0 \frac{\partial^3 u_0}{\partial t^2 \partial x} - I_1 \frac{\partial^4 w}{\partial t^2 \partial x^2} \right] \tag{21}$$

By substituting Eq. (15b) into Eq. (20), we obtain:

$$M = b \left[ \int_{-\frac{h}{2}}^{\frac{h}{2}} z E(z) dz \right] \frac{\partial u_0}{\partial x} - b \left[ \int_{-\frac{h}{2}}^{\frac{h}{2}} z^2 E(z) dz \right] \frac{\partial^2 w}{\partial x^2} + (e_0a)^2 \left[ I_0 \frac{\partial^2 w}{\partial t^2} + I_1 \frac{\partial^3 u_0}{\partial t^2 \partial x} - I_2 \frac{\partial^4 w}{\partial t^2 \partial x^2} + \frac{\partial \bar{N}}{\partial x} \frac{\partial w}{\partial x} + \bar{N} \frac{\partial^2 w}{\partial x^2} \right] \tag{22}$$

Differentiating Eq. (21) once and differentiating Eq. (22) twice with respect to  $x$  and substituting them into Eq. (15a) and (15b), respectively.

$$b \left[ \int_{-\frac{h}{2}}^{\frac{h}{2}} E(z) dz \right] \frac{\partial^2 u_0}{\partial x^2} - b \left[ \int_{-\frac{h}{2}}^{\frac{h}{2}} z E(z) dz \right] \frac{\partial^3 w}{\partial x^3} + (e_0a)^2 \left[ I_0 \frac{\partial^4 u_0}{\partial t^2 \partial x^2} - I_1 \frac{\partial^5 w}{\partial t^2 \partial x^3} \right] = I_0 \frac{\partial^2 u_0}{\partial t^2} - I_1 \frac{\partial^3 w}{\partial t^2 \partial x} \tag{23}$$

$$b \left[ \int_{-\frac{h}{2}}^{\frac{h}{2}} z E(z) dz \right] \frac{\partial^3 u_0}{\partial x^3} - b \left[ \int_{-\frac{h}{2}}^{\frac{h}{2}} z^2 E(z) dz \right] \frac{\partial^4 w}{\partial x^4} + (e_0 a)^2 \frac{\partial^2}{\partial x^2} \left[ I_0 \frac{\partial^2 w}{\partial t^2} + I_1 \frac{\partial^3 u_0}{\partial t^2 \partial x} - I_2 \frac{\partial^4 w}{\partial t^2 \partial x^2} + \frac{\partial \bar{N}}{\partial x} \frac{\partial w}{\partial x} + \bar{N} \frac{\partial^2 w}{\partial x^2} \right] =$$

$$I_0 \frac{\partial^2 w}{\partial t^2} + I_1 \frac{\partial^3 u_0}{\partial t^2 \partial x} - I_2 \frac{\partial^4 w}{\partial t^2 \partial x^2} + \frac{\partial \bar{N}}{\partial x} \frac{\partial w}{\partial x} + \bar{N} \frac{\partial^2 w}{\partial x^2} \quad (1)$$

Boundary condition in both of clamped at ( $x=0$ ), free and simply supported (at  $x=L$ ) are defined as:

Clamped:

$$w(x=0) = 0 \quad (25)$$

$$\frac{\partial w(x=0)}{\partial x} = 0 \quad (26)$$

Free:

$$M(x=L) = 0 \quad (27)$$

$$\frac{\partial M(x=L)}{\partial x} = 0 \quad (28)$$

Simply Supported:

$$w(x=L) = 0 \quad (29)$$

$$M(x=L) = 0 \quad (30)$$

### 3 SOLUTION PROCEDURE

In this study GDQ method is used to calculate the spatial derivatives of field variables in equilibrium equations. In implementation of GDQ, Grid points describe the locations of calculating derivatives and field variables. Derivative of a function with respect to a variable at a given node is calculated as a weighted linear sum of the function values at all nodes in the mesh line. Thus, we can define the " $r$ -th" order derivative of a function " $f(x)$ " as linear sum of the function values which is (Shu [26]):

$$\left. \frac{\partial^r f(x)}{\partial x^r} \right|_{x=x_p} = \sum_{j=1}^n C_{ij}^{(r)} f(x_j) \quad (31)$$

That  $n$  is the number of grid points along  $x$  direction and  $C_{ij}$  can be obtained by following equation:

$$C_{ij}^{(1)} = \frac{M(x_i)}{(x_i - x_j)M(x_j)}; \quad i, j = 1, 2, \dots, n \quad \text{and} \quad i \neq j$$

$$C_{ij}^{(1)} = - \sum_{j=1, j \neq i}^n C_{ij}^{(1)}; \quad i = j \quad (32)$$

where  $M(x)$  is defined as:

$$M(x_i) = \prod_{j=1, j \neq i}^n (x_i - x_j) \tag{33}$$

The weighting coefficient along  $x$  direction  $C^{(r)}$  can be obtained as:

$$C_{ij}^{(r)} = r \left[ C_{ij}^{(r-1)} C_{ij}^{(1)} - \frac{C_{ij}^{(r-1)}}{(x_i - x_j)} \right]; \quad i, j = 1, 2, \dots, n, i \neq j \quad \text{and} \quad 2 \leq r \leq n-1 \tag{34}$$

$$C_{ii}^{(r)} = - \sum_{j=1, j \neq i}^n C_{ij}^{(r)}; \quad i, j = 1, 2, \dots, n \quad \text{and} \quad 1 \leq r \leq n-1$$

To obtain a better distribution for mesh point, Chebyshev-Gauss-Lobatto technique is applied as (Civalek [6]):

$$x_i = \frac{L}{2} \left( 1 - \cos \left( \frac{(i-1)}{(N-1)} \pi \right) \right) \quad i = 1, 2, 3, \dots, n \tag{35}$$

In fact, by using this distribution, increased convergence speed of solutions can be achieved. Finally, according to the DQ method, the governing Eqs. (23), (24) should also be re-written in discretized form. In terms of generalized differential quadrature, the governing differential equation is expressed by:

$$\begin{aligned} & \sum_{s=1}^n C_{rs}^{(1)} \left[ b \left[ \int_{-\frac{h}{2}}^{\frac{h}{2}} E(z) dz \right] \sum_{s=1}^n C_{rs}^{(1)} U_s \right] - \sum_{s=1}^n C_{rs}^{(1)} \left[ b \left[ \int_{-\frac{h}{2}}^{\frac{h}{2}} z E(z) dz \right] \sum_{s=1}^n C_{rs}^{(2)} W_s \right] \\ & = \omega^2 \left[ m_0 U_s - m_1 \sum_{s=1}^n C_{rs}^{(1)} W_s - (e_0 a)^2 \sum_{s=1}^n C_{rs}^{(2)} \left( m_0 U_s - m_1 \sum_{s=1}^n C_{rs}^{(1)} W_s \right) \right] \\ & - \sum_{s=1}^n C_{rs}^{(2)} \left[ b \left[ \int_{-\frac{h}{2}}^{\frac{h}{2}} z^2 E(z) dz \right] \sum_{s=1}^n C_{rs}^{(2)} W_s - b \left[ \int_{-\frac{h}{2}}^{\frac{h}{2}} z E(z) dz \right] \sum_{s=1}^n C_{rs}^{(1)} U_s \right] \\ & + \sum_{s=1}^n C_{rs}^{(1)} \left( N^x \sum_{s=1}^n C_{rs}^{(1)} W_s \right) - (e_0 a)^2 \sum_{s=1}^n C_{rs}^{(2)} \left[ \sum_{s=1}^n C_{rs}^{(1)} \left( N^x \sum_{s=1}^n C_{rs}^{(1)} W_s \right) \right] \\ & = \omega^2 \left\{ m_0 W_s + m_1 \sum_{s=1}^n C_{rs}^{(1)} U_s - m_2 \sum_{s=1}^n C_{rs}^{(2)} W_s - (e_0 a)^2 \sum_{s=1}^n C_{rs}^{(2)} \left[ \begin{matrix} m_0 W_s + m_1 \sum_{s=1}^n C_{rs}^{(1)} U_s \\ -m_2 \sum_{s=1}^n C_{rs}^{(2)} W_s \end{matrix} \right] \right\} \end{aligned} \tag{36}$$

$$\tag{37}$$

Every term of motion equation can be transformed to sum of many nodal weighted residuals of variables and by using differential quadrature method, it can be written as a discretized form. Therefore, by considering the transverse displacement in the form of  $w = W e^{i\omega t}$ , discrete differential motion equation of model would be transformed to some algebraic terms

$$\begin{bmatrix} [A_{bb}] & [A_{bi}] \\ [A_{ib}] & [A_{ii}] \end{bmatrix} \begin{Bmatrix} W_b \\ W_i \end{Bmatrix} = \omega^2 \begin{bmatrix} 0 & 0 \\ [B_{ib}] & [B_{ii}] \end{bmatrix} \begin{Bmatrix} W_b \\ W_i \end{Bmatrix} \tag{38}$$

where subtitles  $b$  represent the grid nodes in the border and adjacent areas that the boundary conditions are applied and subtitles  $i$  denote other grid nodes.

## 4 NUMERICAL RESULTS

### 4.1 Validation

In this section, numerical results are presented for vibration behavior of both cantilever and propped cantilever nano-beams with rotary effect, thermal effect, non-dimensional angular velocity and length scale parameter effects investigation. To do this, we use the Euler-Bernoulli beam model based on Eringen's theory. To get better understanding of results, the governing equation has to be transformed to non-dimensional form. By the way, the following variable changes is needed:

$$\begin{aligned} x &= \xi L; & r &= \delta L; & \Phi^2 &= \left( \frac{m_0}{EI} \right)_{ceramic} L^4 \Omega^2; \\ \Psi^2 &= \left( \frac{m_0}{EI} \right)_{ceramic} L^4 \omega^2; & \left( \frac{m_0}{EI} \right)_{ceramic} &= \frac{12 \rho_{ceramic}}{E_{ceramic} h_1^2}; & \mu &= \frac{e_0 a}{L} \end{aligned} \quad (39)$$

where  $\Phi$ ,  $\Psi$ ,  $\mu$  are non-dimensional angular velocity, frequency and nonlocal parameter, respectively. In order to obtain accurate and convergent results for DQ method, sufficient number of grid points (fifteen) is required. As it can be seen in Table 2., for accuracy and the efficiency verification of numerical analysis, the current results are compared with the results presented by (Aranda-Ruiz et al., [1], Narendar [23], Pradhan and Murmu[24]). To verify accuracy of the results, the non-dimensional frequency of non-rotating cantilever and propped cantilever nano-beams are compared with results obtained by Lu et al. [18], Wang et al. [33] and Ebrahimi and Salari [8] in Table 3., Table 4 and Table 5., respectively. Also, comparison of non-dimensional frequency of rotating nano-beam for two nonlocal parameters i.e. " $\mu = 0, 0.2$ " and result of Aranda-Ruiz et al.[1] are shown in Fig. 2.

**Table 2**

The effect of the number of grid points on evaluating the non-dimensional natural frequency of the cantilever nano-beam with considering the nonlocal scale parameter.

Nonlocal parameter ( $\mu$ )	Grid points ( $N$ )				
	$N=12$	$N=14$	$N=15$	$N=17$	$N=18$
0	1.874972918	1.875104	1.875104	1.875104	1.875104
0.1	1.878279493	1.879163	1.879173	1.879173	1.879173
0.2	1.888786935	1.891905	1.891938	1.891938	1.891938
0.3	1.908580147	1.915331	1.915199	1.915199	1.915199
0.4	1.942707597	1.954241	1.963253	1.963253	1.963253
0.5	2.005378872	2.021512	2.011347	2.011347	2.011347

**Table 3**

Comparison of results for non-dimensional frequency, of cantilever nano-beam  $\sqrt{\Psi}$

Nonlocal parameter ( $\mu$ )	$\Phi = 0$	
	Present	Wang et al. [33]
0	1.8751041	1.8751041
0.1	1.8791728	1.8791728
0.2	1.8919383	1.8919383
0.3	1.915199	1.915199
0.4	1.9632529	1.9632529
0.5	2.0113471	2.0113471

**Table 4**

Comparison of results for non-dimensional frequency,  $\sqrt{\Psi}$  of propped cantilever nano-beam.

Nonlocal parameter ( $\mu$ )	$\Phi = 0$	
	Present	Lu et al. [18]
0	3.9266	3.9266
0.1	3.820918	3.8209
0.3	3.283001	3.2828
0.5	2.790175	2.7899
0.7	2.439413	2.4364

**Table 5**  
Comparison of results for non-dimensional frequency,  $\Psi$  of propped cantilever FG nano-beam, ( $\mu=0, \Delta T=0$ ).

FG index, ( $n$ )	$\Phi=0, \Psi_1$		$\Phi=0, \Psi_2$	
	Present GDQM (Euler-Bernoulli)	Ebrahimi and Salari[8] (Analytical)	Present GDQM (Euler-Bernoulli)	Ebrahimi and Salari[8] (Analytical)
0	15.33968	15.3397	49.74309	49.7431
0.2	13.56476	13.5647	43.80938	43.8094
1	11.03362	11.0336	35.63681	35.6368
5	9.44947	9.4494	30.52862	30.5286

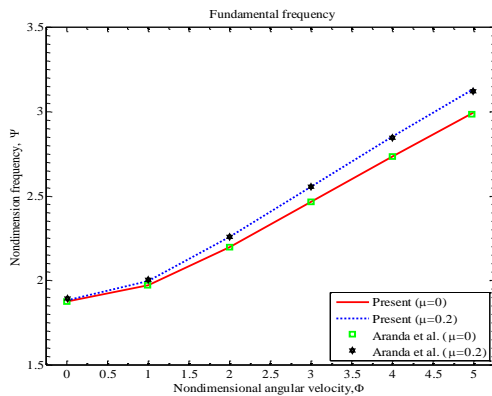


**Fig. 2**  
Comparison of the non-dimensional frequency of rotating micro-beam with the results obtained by Aranda-Ruiz et al.[1].

### 4.2 Results and discussion

After extensive validation of the presented formulation, the effects of different parameters on the vibration of FG rotating nano-beam such as: nonlocal parameter, gradient index, non-dimensional angular velocity, hub radius and temperature change are investigated. The variations of the three first modes of non-dimensional frequencies of nano-cantilever and nano propped cantilever beams, with thermal variation for different values of the nonlocal parameter  $\mu$  and different values of non-dimensional angular velocity parameter  $\Phi$ , which represents the gradient index  $n$ , will be figured out. For the nonlocal model,  $\mu$  can be 0, 0.1, 0.2, 0.3, 0.4 and 0.5. The rotating non-dimensional angular velocity,  $\Phi$ , hub radius,  $\delta$ , and gradient index,  $n$ , are assumed to be in the range of (0–5), (0, 1, 4, 8) and (0, 0.25, 0.5, 1), respectively. The bottom surface of the beam is pure steel, while the top surface of the beam is ceramic. Beam geometry is:  $h$  (thickness) = 3.4 nm,  $b$  (width) =  $h$  and  $L$  (width) = 10 $h$ . The results are obtained by using GDQM. In this section the results and considerations regarding the boundary conditions can be divided into two parts of cantilever and propped cantilever.

#### 4.2.1 Cantilever

Variations of the non-dimensional fundamental frequency of the cantilever FG nano-beam with respect to non-dimensional angular velocity for different values of gradient indexes and nonlocal parameters are illustrated in Fig. 3. It is observed that, for both the local and nonlocal models, the non-dimensional fundamental frequency increases with increasing the nonlocal parameter. Frequencies by local and nonlocal models are close to each other at low angular velocities and due to increasing the inertia, both of them increase with the value of angular velocity. Variation of the second and third non-dimensional frequencies with the non-dimensional angular velocity for different values of nonlocal parameters and gradient indexes are show in Figs. 4 and 5. Opposite to the fundamental frequency, for second and third modes, as  $\mu$  increases, the frequencies observed by nonlocal models are smaller to that of local ones. In higher non-dimensional angular velocity, the effects of nonlocal parameter on the frequencies reduce and the frequency decreases with increasing FG index. With increasing angular velocity, a axial tensile force is applied to nano-beam and due to this force, stiffness of nano-beam increases. Therefore increase of stiffness causes increase of natural frequency. Figs. 6-8 illustrate first three modes of non-dimensional frequencies versus the gradient index for different values of nonlocal parameters and angular velocity. By changing the gradient index parameter and fixing the nonlocal parameter, results are decreasing in the non-dimensional frequencies for each

angular velocity. That is because of the nano-beam stiffness due to ceramics phase constituent increase. However, increasing the nonlocal parameter causes the fundamental frequency increase, at a constant material distribution. It is noticeable that, the non-dimensional frequency reduces with high rate where the gradient index is in the range of 0 to 1 in comparison with gradient index in a higher range. In addition to local model, first three non-dimensional frequency modes decrease with high rate rather than nonlocal model. Fig. 9 shows the variations of the non-dimensional fundamental frequency of the cantilever FG nano-beam with respect to temperature change for different values of gradient indexes and nonlocal parameters for  $\Phi = 2$ . It is seen from this figure that, for both the local and nonlocal models, the fundamental non-dimensional frequency increases with increasing the temperature and with rising the nonlocal parameter the frequency increases. It is deduced that, with rising gradient index and the subsequent reduction of stiffness, the frequency decreases. Fig. 10 illustrates the second dimensionless frequency versus temperature changes for different values of gradient and nonlocal parameter. It can be seen, from Fig. 10, that an increase in the temperature change causes a decrease in the natural frequency of the nano-beam. This is because of the fact that an increase in temperature change leads to a decrease in the stiffness of nano-beam, and causes a decrease in natural frequency. Also, as the value of gradient index increases, this leads to a decrease in the dimensionless natural frequency of the nano-beam. Fig. 11 presents a similar trend. When one draws a comparison between Figs. 10 and 11, it can be inferred that while the mode number changes from second to third, the natural frequency increases. Figs. 12 to 14 display the variation of the first, second and third non-dimensional frequencies with respect to the temperature changes with angular velocity and hub radius variations for  $n=0.2$ . It is observable that, the first three non-dimensional frequencies increase by increasing the non-dimensional angular velocity. Opposite the first mode that frequency increases with increasing the temperature, at second and third modes the frequency reduces with increasing the temperature. As the hub radius increases, variation of frequency through the temperature change increases.

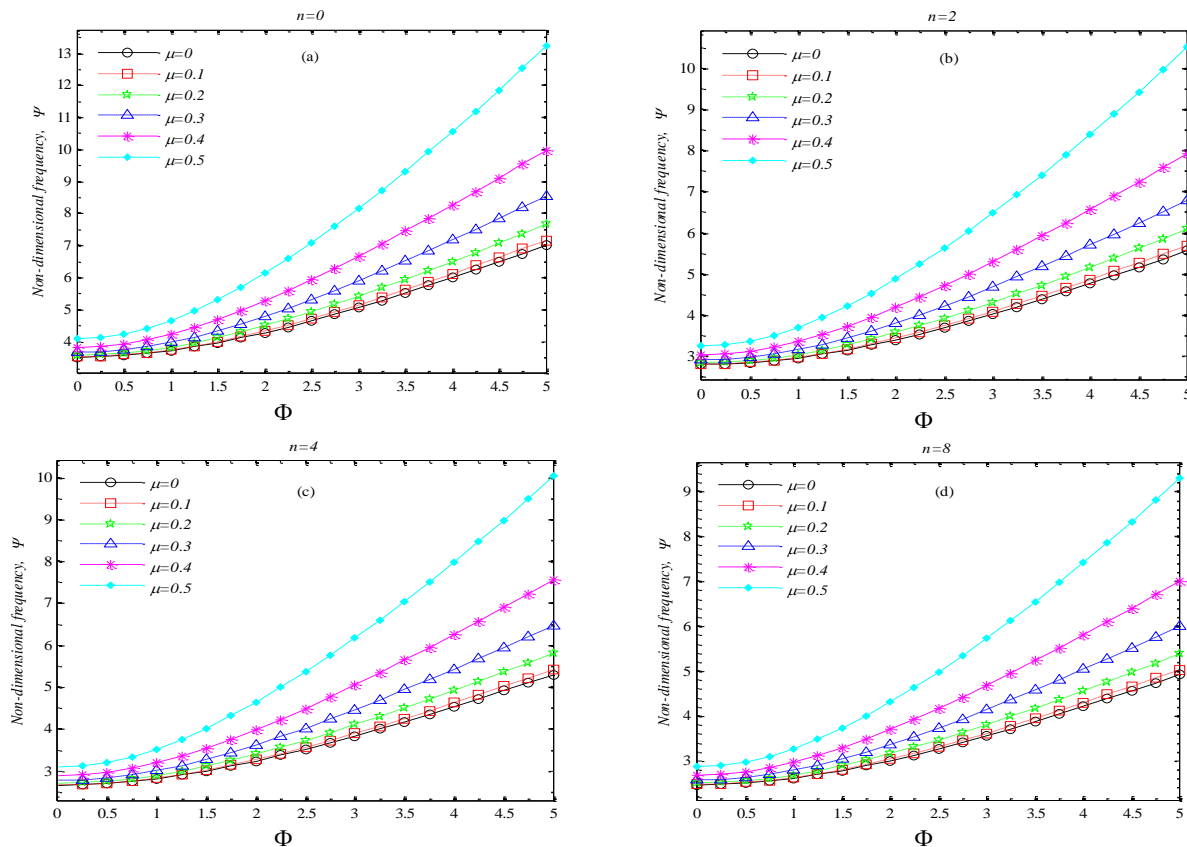


**Fig. 3** Variations of the fundamental non-dimensional frequency of the cantilever FG nano-beam with respect to non-dimensional angular velocities for different values of nonlocal parameters and gradient indexes,  $\delta=0.25$ ,  $h=b/2=L/20=0.5$  (nm).

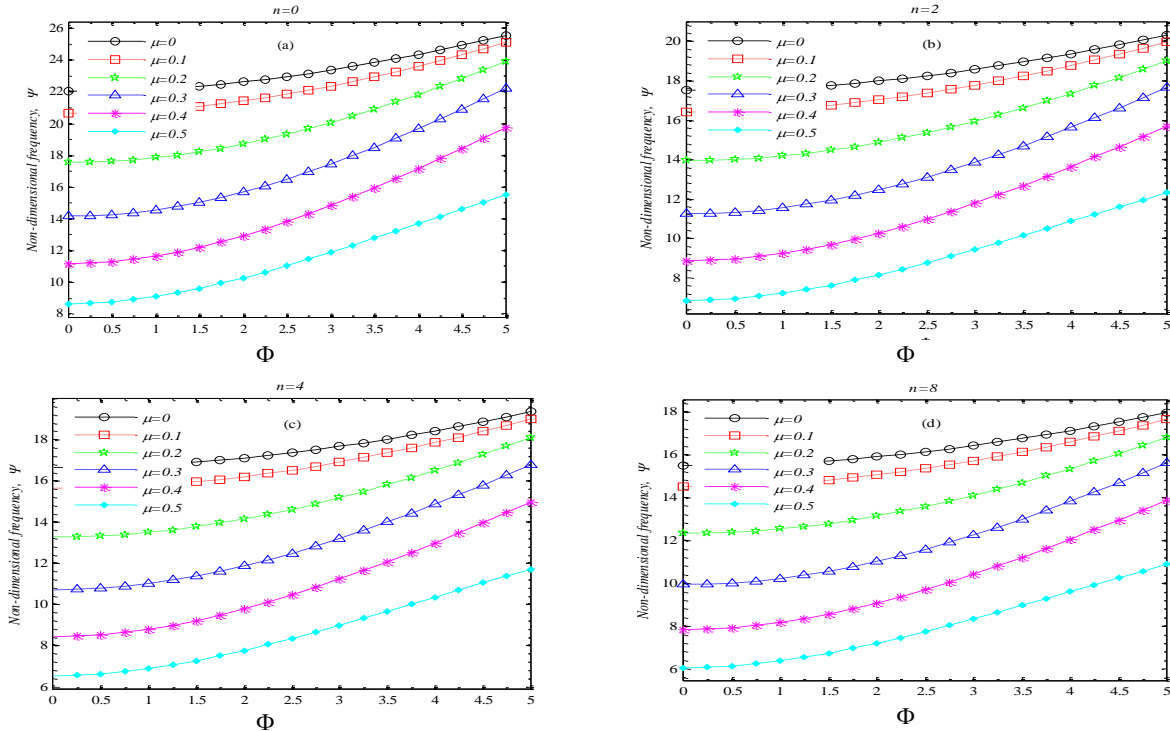


**Fig. 4** Variations of the second non-dimensional frequency of the cantilever FG nano-beam with respect to non-dimensional angular velocities for different values of nonlocal parameters and gradient indexes,  $\delta=0.25$ ,  $h=b/2=L/20=0.5$  (nm).

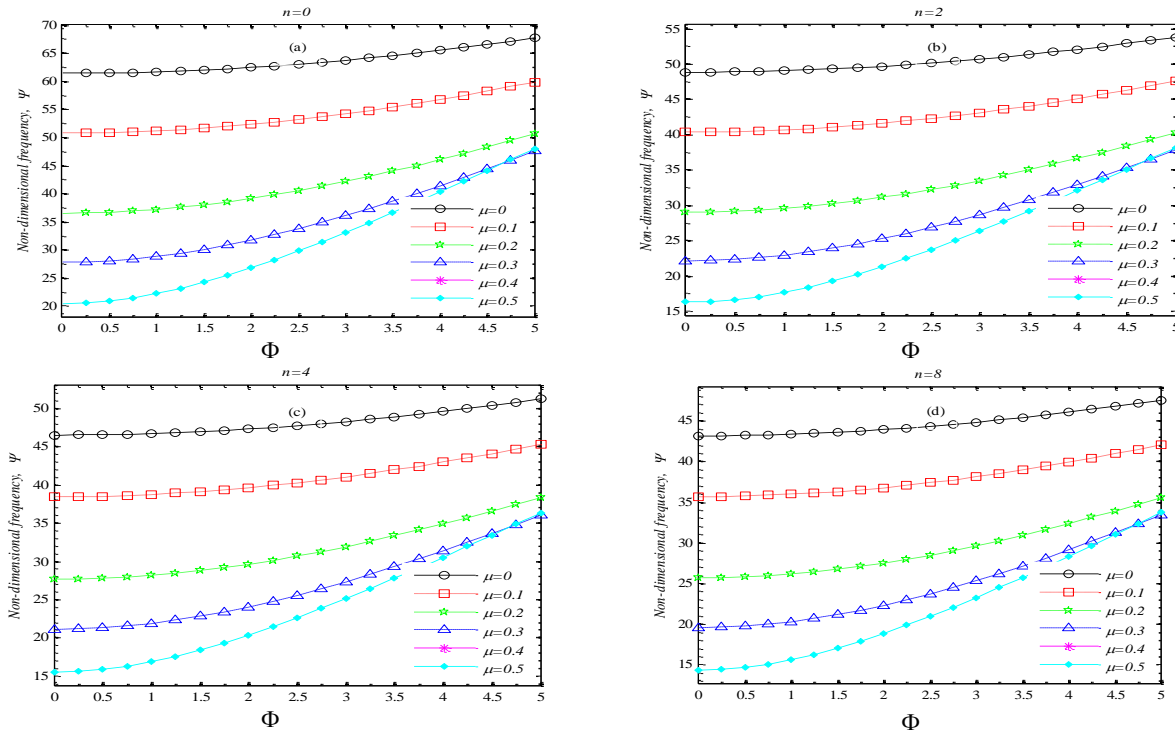


**Fig. 5** Variations of the third non-dimensional frequency of the cantilever FG nano-beam with respect to non-dimensional angular velocities for different values of nonlocal parameters and gradient indexes,  $\delta=0.25$ ,  $h=b/2=L/20=0.5$  (nm).

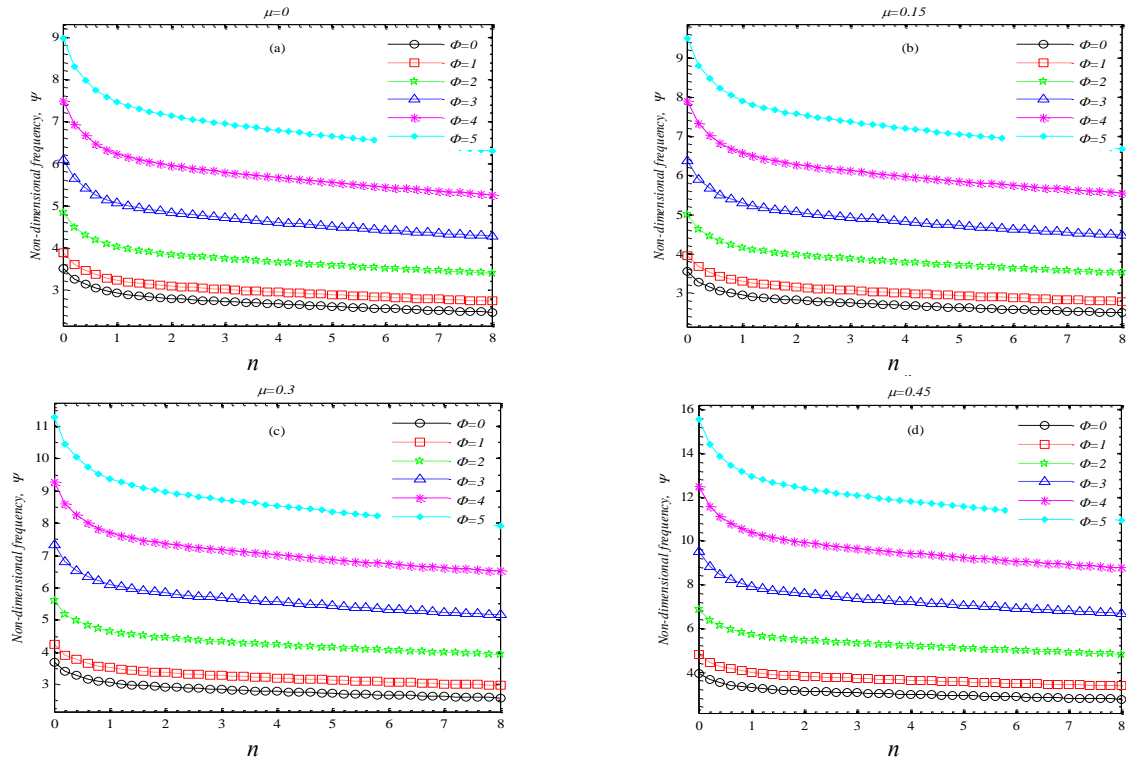


**Fig. 6** Variations of the fundamental non-dimensional frequency of the cantilever FG nano-beam with respect to gradient indexes for different values of nonlocal parameters and non-dimensional angular velocities,  $\delta=1$ ,  $h=b/2=L/20=0.5$  (nm).

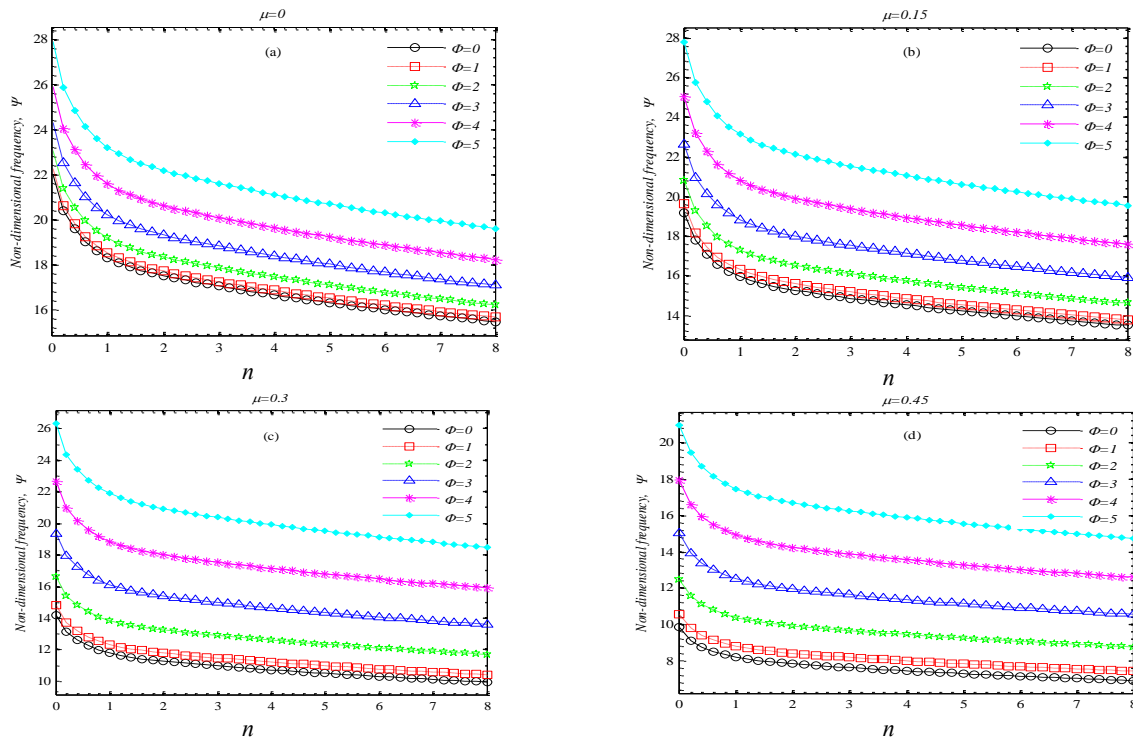


**Fig. 7** Variations of the second non-dimensional frequency of the cantilever FG nano-beam with respect to gradient indexes for different values of nonlocal parameters and non-dimensional angular velocities,  $\delta=1$ ,  $h=b/2=L/20=0.5$  (nm).

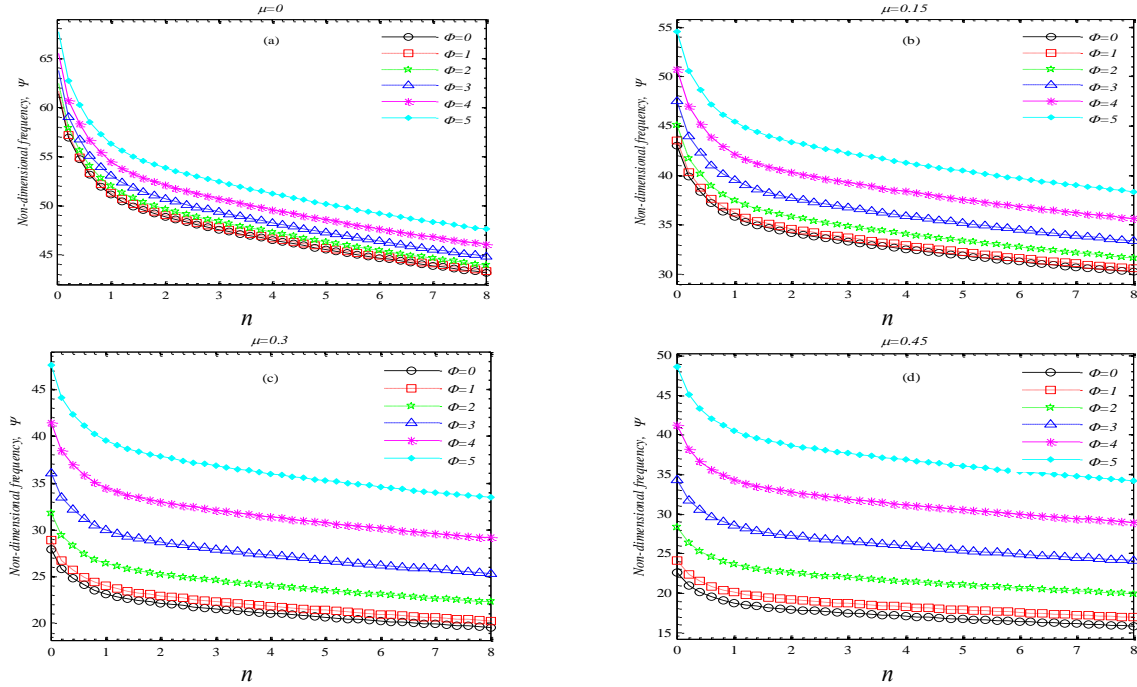


**Fig. 8** Variations of the third non-dimensional frequency of the cantilever FG nano-beam with respect to gradient indexes for different values of nonlocal parameters and non-dimensional angular velocities,  $\delta=1, h=b/2=L/20=0.5$  (nm).

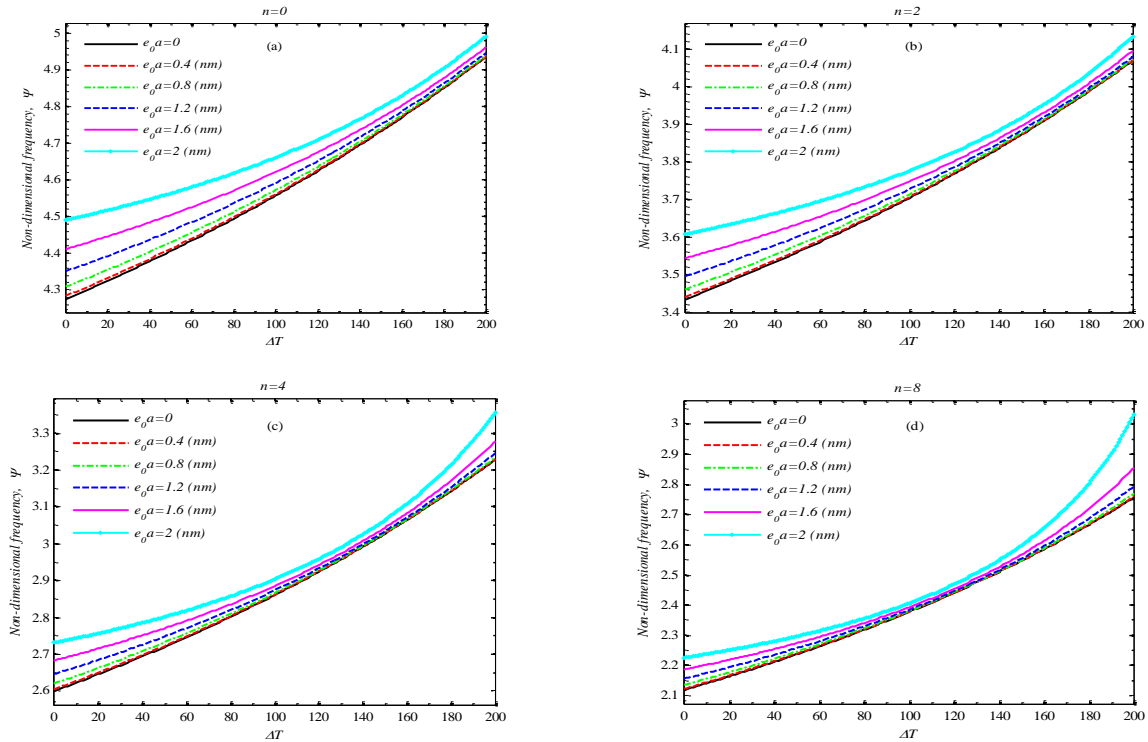


**Fig. 9** Variations of the fundamental non-dimensional frequency of the cantilever FG nano-beam with respect to temperature change for different values of gradient indexes and nonlocal parameters,  $h=b/L/20=0.5$  (nm),  $\Phi=2$ .

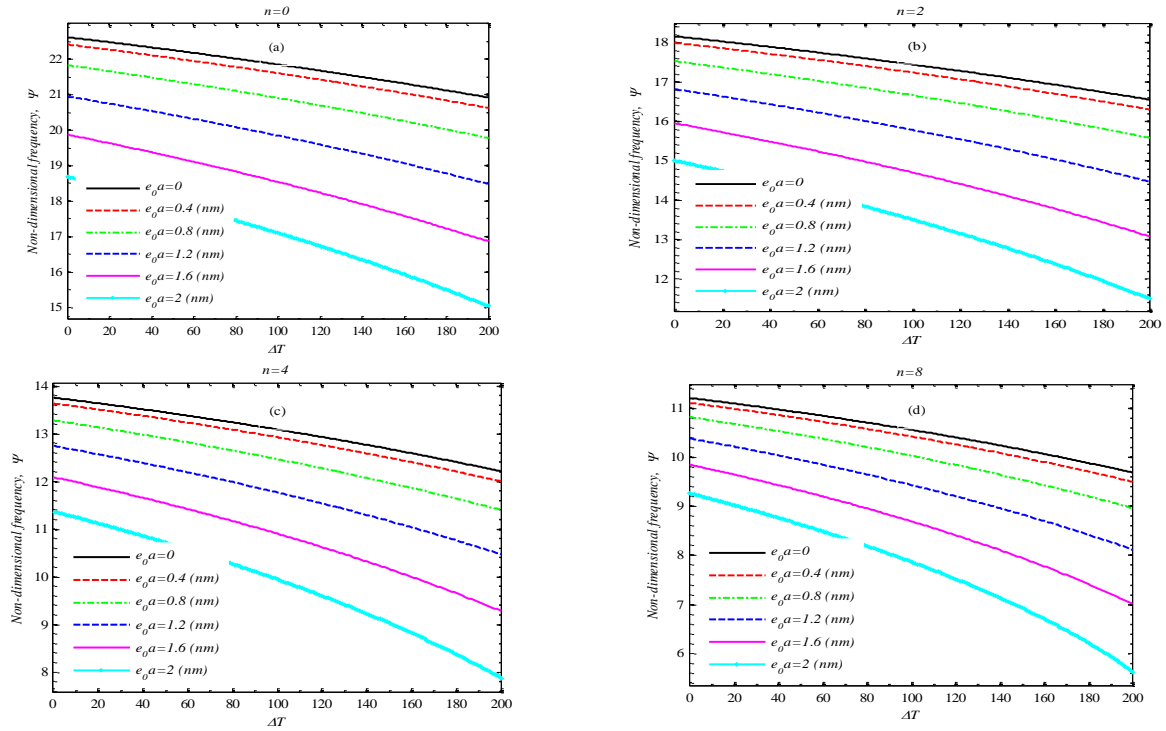


**Fig. 10** Variations of the second non-dimensional frequency of the cantilever FG nano-beam with respect to temperature change for different values of gradient indexes and nonlocal parameters,  $h=b=L/20=0.5$  (nm),  $\Phi=2$ .

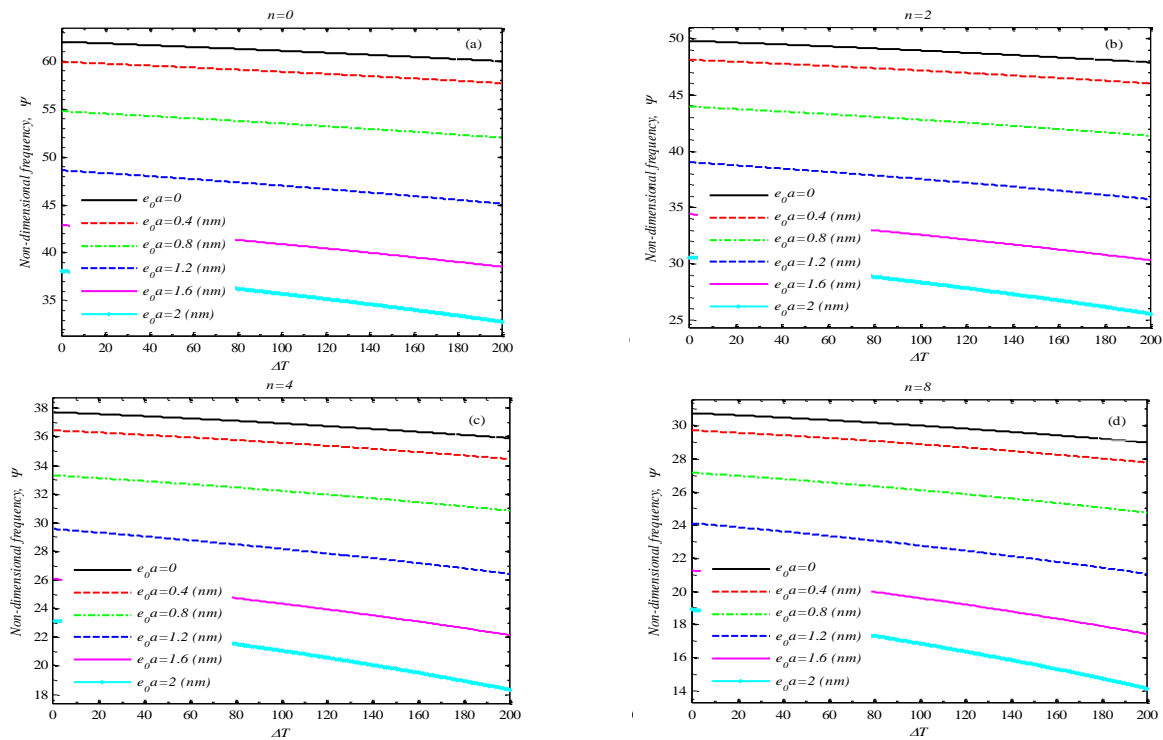


**Fig. 11** Variations of the third non-dimensional frequency of the cantilever FG nano-beam with respect to temperature change for different values of gradient indexes and nonlocal parameters,  $h=b=L/20=0.5$  (nm),  $\Phi=2$ .

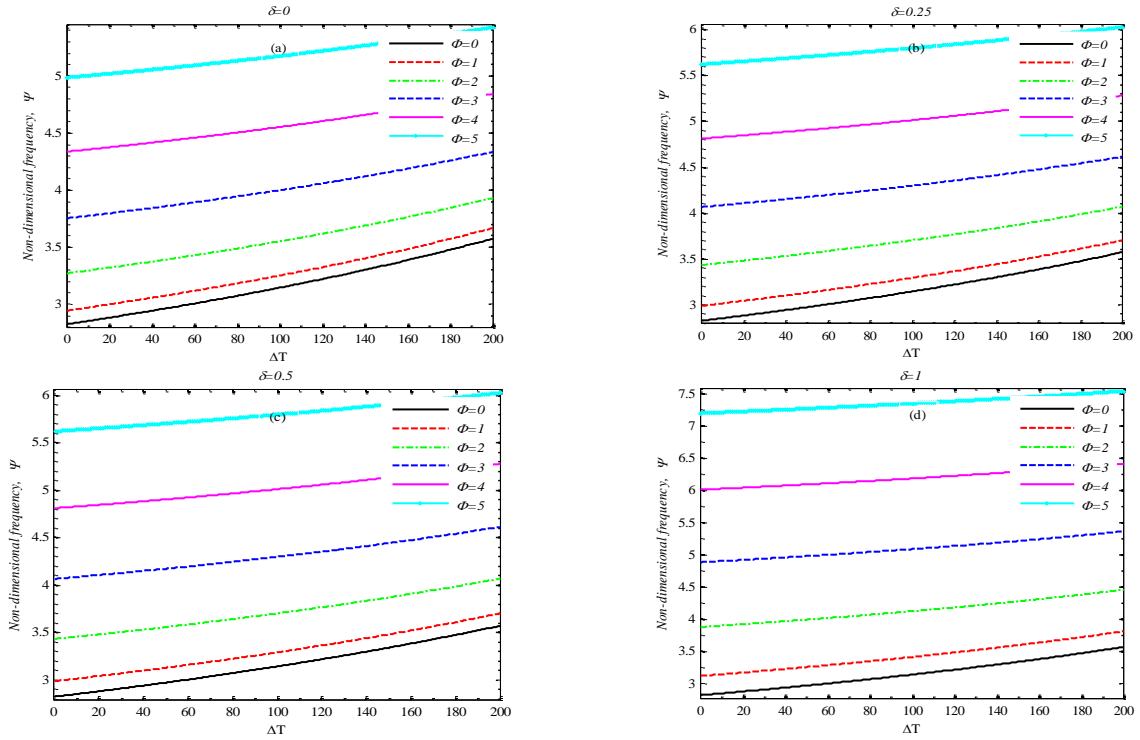


**Fig. 12** Variations of the fundamental non-dimensional frequency of the cantilever FG nano-beam with respect to temperature change for different values of hub radius and non-dimensional angular velocities,  $h=b/4=L/40=0.25$  (nm) and  $n=0.2$ .

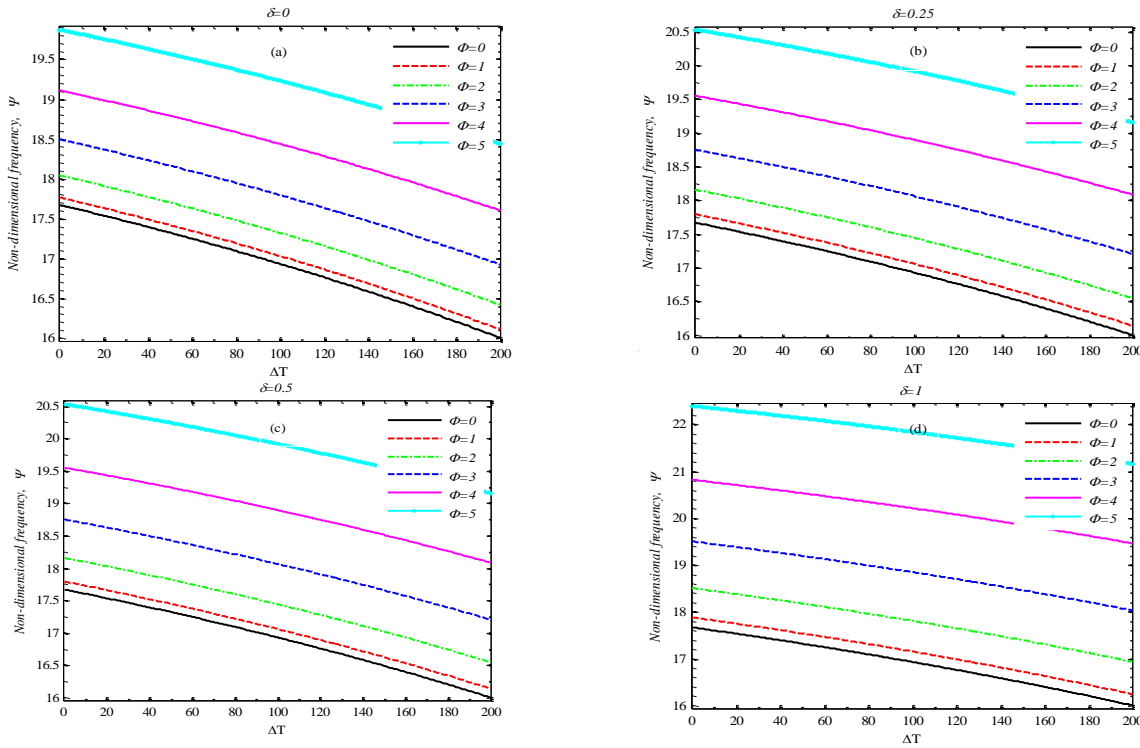


**Fig. 13** Variations of the second non-dimensional frequency of the cantilever FG nano-beam with respect to temperature change for different values of hub radius and non-dimensional angular velocities,  $h=b/4=L/40=0.25$  (nm) and  $n=0.2$ .

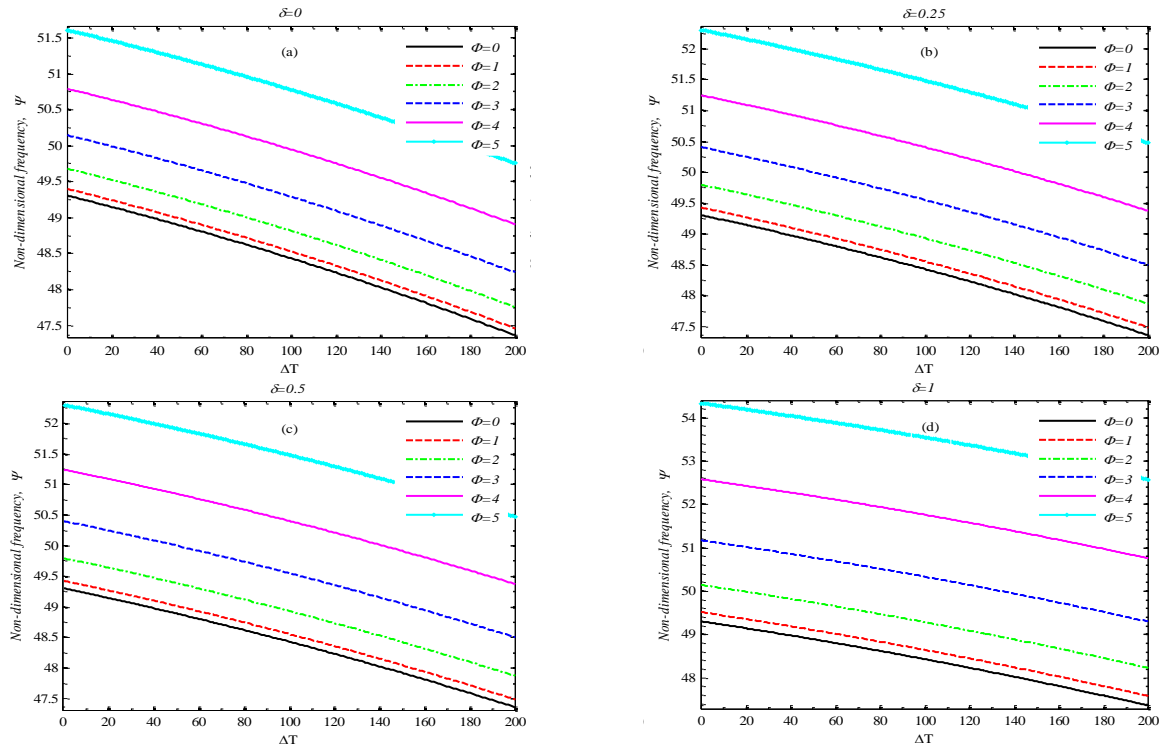


**Fig. 14**

Variations of the third non-dimensional frequency of the cantilever FG nano-beam with respect to temperature change for different values of hub radius and non-dimensional angular velocities,  $h=b/4=L/40=0.25$  (nm) and  $n=0.2$ .

#### 4.2.2 Propped cantilever

Figs.15 to 17 show the first three modes of non-dimensional frequencies versus the non-dimensional angular velocity for different values of nonlocal parameters and gradient indexes. Opposite to the cantilever nano-beam, for both the local and nonlocal models, the non-dimensional frequency decreases with increasing the nonlocal parameter and frequencies by local and nonlocal models are close to each other at high angular velocities and both of them increase with the value of angular velocity. Second and third frequency are similar to frequency of cantilever nano-beam. Figs. 18 to 20 show the variation of non-dimensional first, second and third frequency with respect to gradient index. Similar deductions can be obtained for different values of nonlocal parameter and non-dimensional angular velocity. Variations of the first three non-dimensional frequencies of the propped cantilever FG nano-beam  $s$  with respect to temperature changes for different values of gradient indexes and nonlocal parameters are depicted in Figs. 21-23, respectively. It is observed from the figures that, frequencies of propped cantilever FG nano-beam decrease with increasing the temperature until it approaches to the critical temperature. This is because of the reduction stiffness of the beam. When temperature rises, the geometrical stiffness decreases and frequency arrives to lowest value at the critical temperature point. After the branching point, frequency starts to increase. It is noticed that the propped cantilever nano-beam  $s$  with lower value of nonlocal parameter make larger values of the frequency results. It is discernible that, with increasing the gradient index, the branching point is created at lower temperature, because at the lower gradient indexes, the structure stiffness will be more. Finally, variations of the first, second and third non-dimensional frequency of the propped cantilever FG nano-beam with temperature change for different values of hub radius and non-dimensional angular velocities for  $n=0.2$ . are shown in Figs. 24-26. In these figures opposite to the Figs.21 to 23, propped cantilever nano-beam  $s$  with higher value of nonlocal parameter make larger values of the frequency results and with increasing hub radius, the branching point is created at higher temperature.

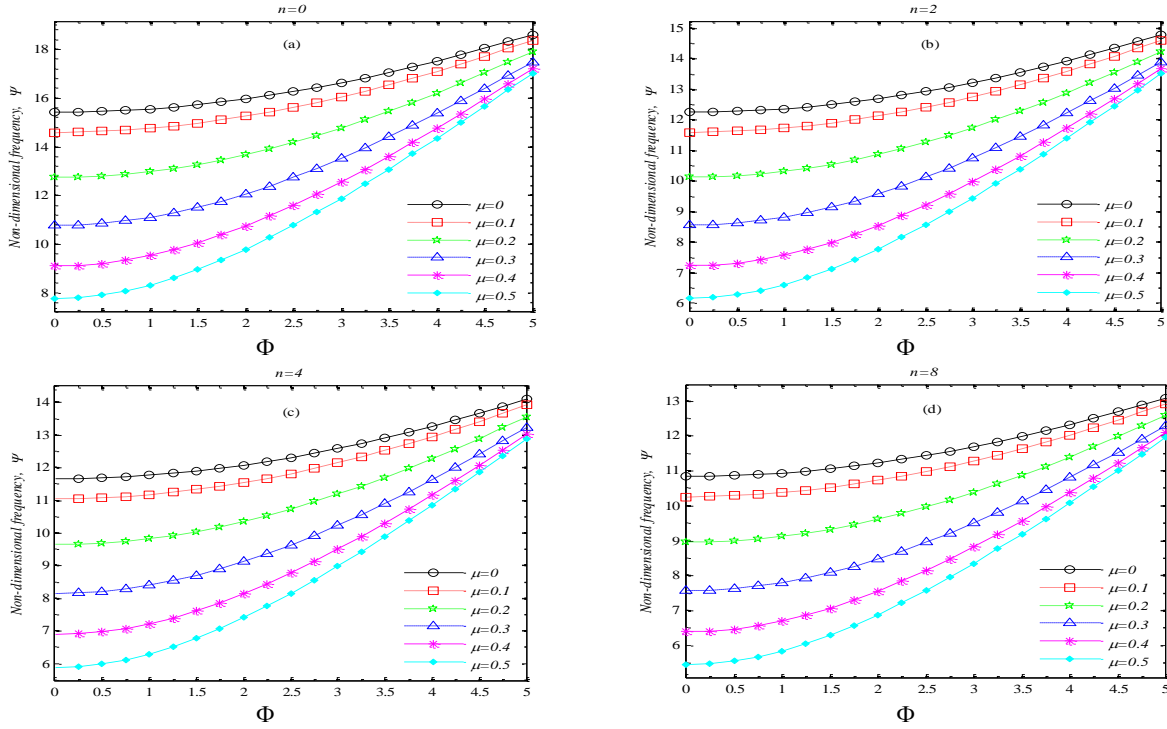


**Fig. 15** Variations of the fundamental non-dimensional frequency of the propped cantilever FG nano-beam with respect to non-dimensional angular velocities for different values of nonlocal parameters and gradient indexes,  $\delta=0.25$ ,  $h=b/2=L/20=0.5$  (nm).

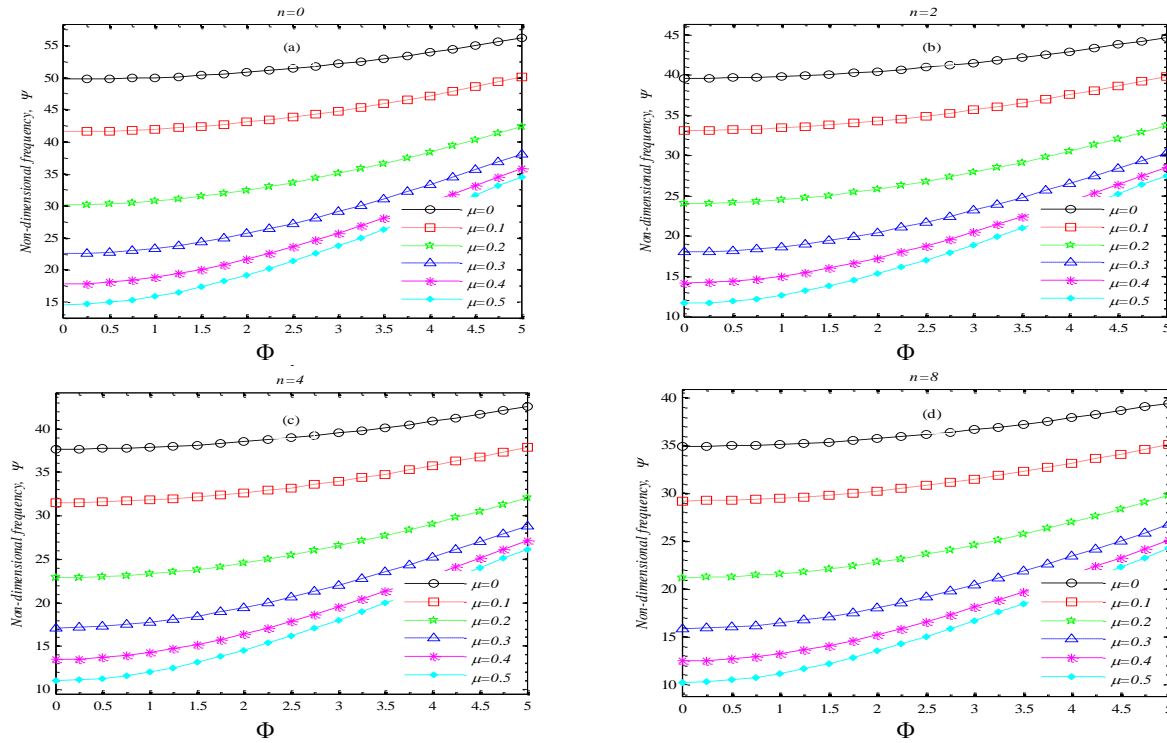


**Fig. 16** Variations of the second non-dimensional frequency of the propped cantilever FG nano-beam with respect to non-dimensional angular velocities for different values of nonlocal parameters and gradient indexes,  $\delta=0.25$ ,  $h=b/2=L/20=0.5$  (nm).

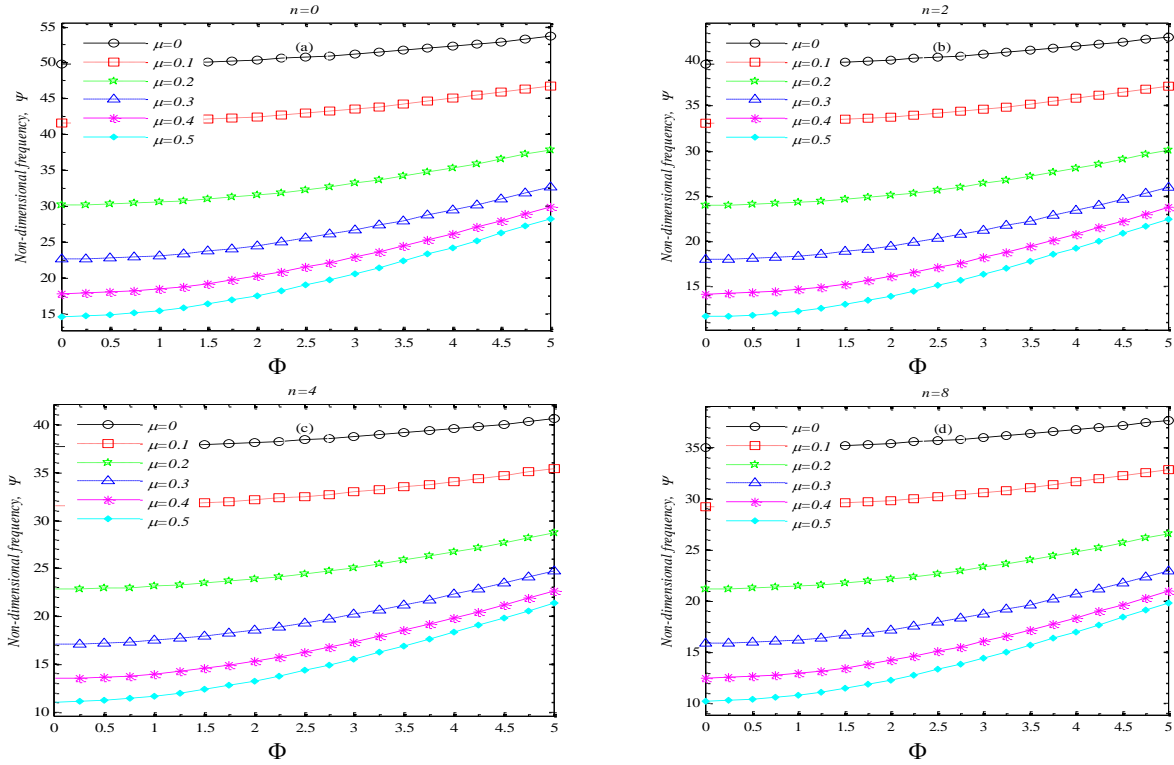


**Fig. 17** Variations of the third non-dimensional frequency of the propped cantilever FG nano-beam with respect to non-dimensional angular velocities for different values of nonlocal parameters and gradient indexes,  $\delta=0.25$ ,  $h=b/2=L/20=0.5$  (nm).

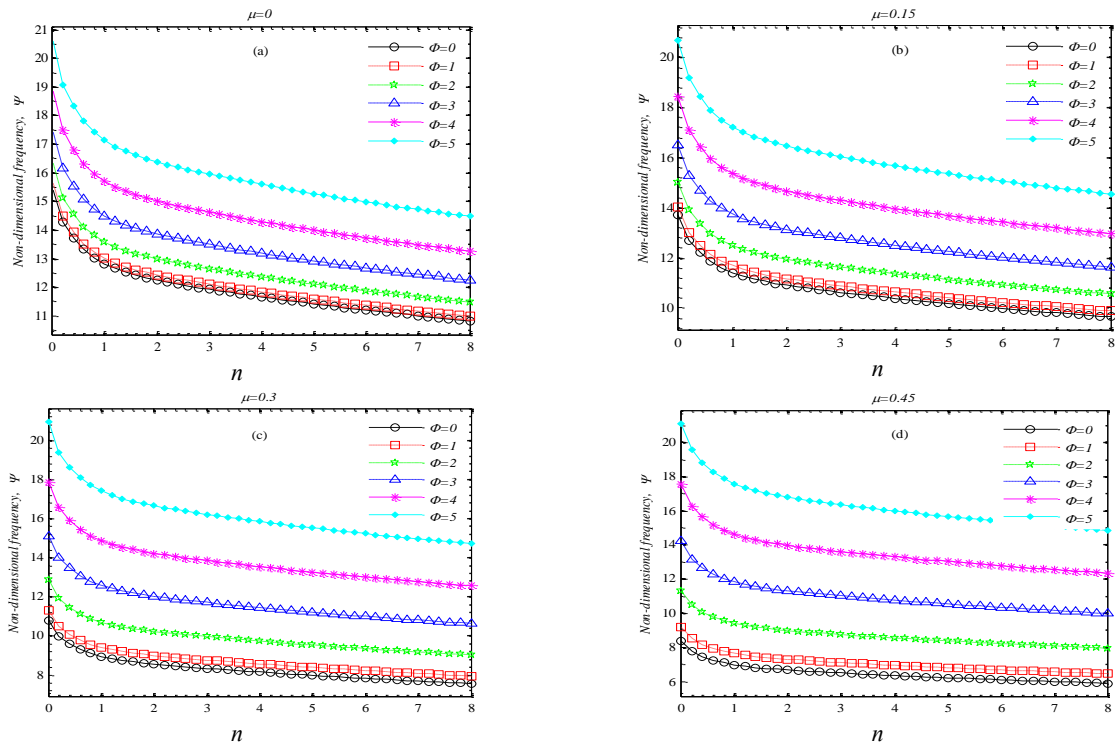


**Fig. 18** Variations of the fundamental non-dimensional frequency of the propped cantilever FG nano-beam with respect to gradient indexes for different values of nonlocal parameters and non-dimensional angular velocities,  $\delta=1$ ,  $h=b/2=L/20=0.5$  (nm).

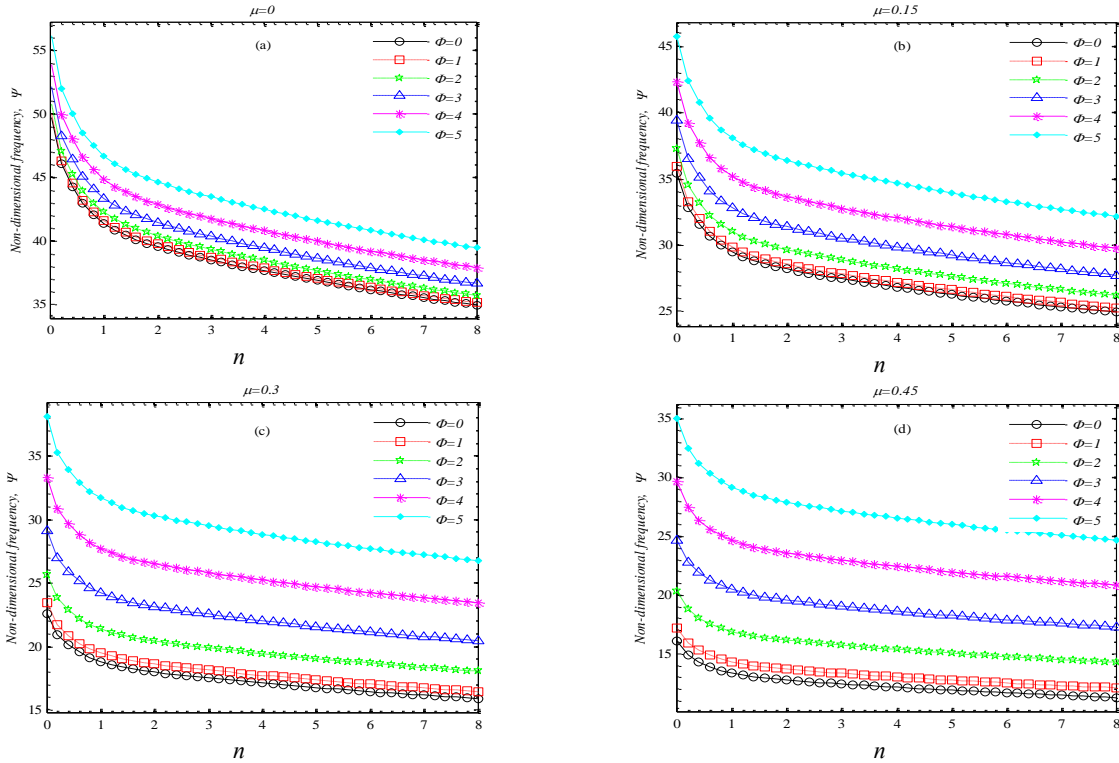


**Fig. 19** Variations of the second non-dimensional frequency of the propped cantilever FG nano-beam with respect to gradient indexes for different values of nonlocal parameters and non-dimensional angular velocities,  $\delta=1$ ,  $h=b/2=L/20=0.5$  (nm).

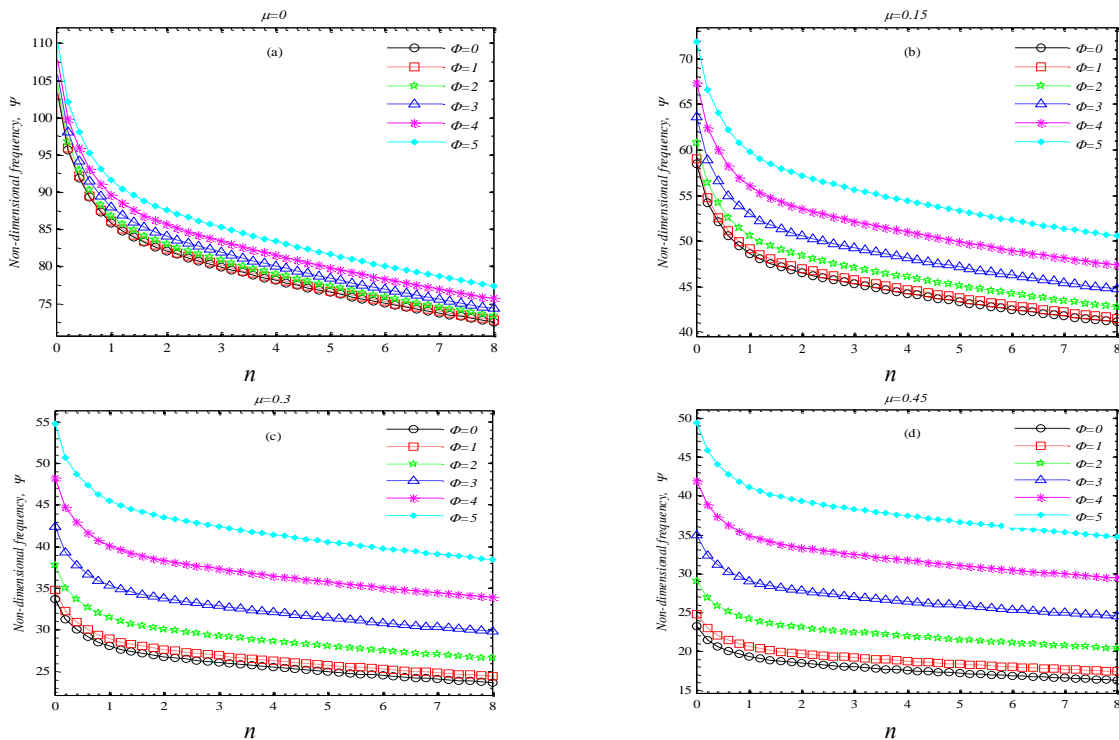


**Fig. 20** Variations of the third non-dimensional frequency of the propped cantilever FG nano-beam with respect to gradient indexes for different values of nonlocal parameters and non-dimensional angular velocities,  $\delta=1$ ,  $h=b/2=L/20=0.5$  (nm).

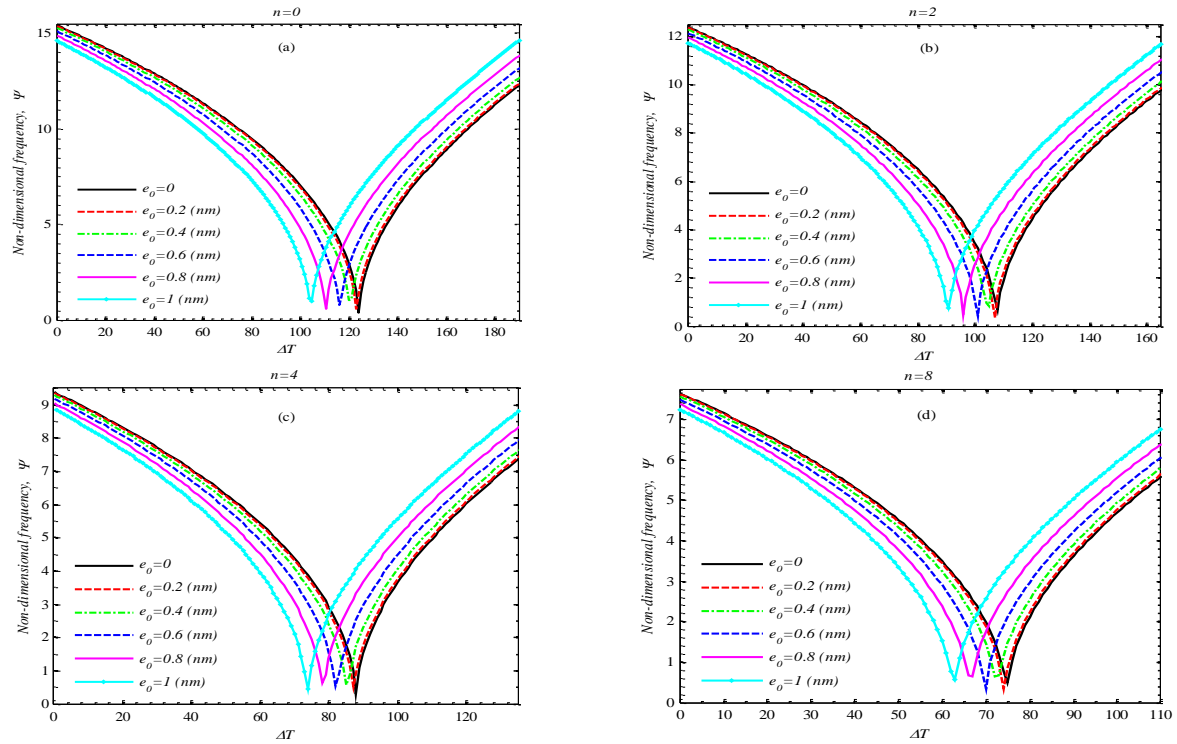


**Fig. 21** Variations of the fundamental non-dimensional frequency of the propped cantilever FG nano-beam with respect to temperature change for different values of gradient indexes and nonlocal parameters,  $h=2b/5=L/50=0.2$  ( $n$ ) and  $\Phi=0$ .

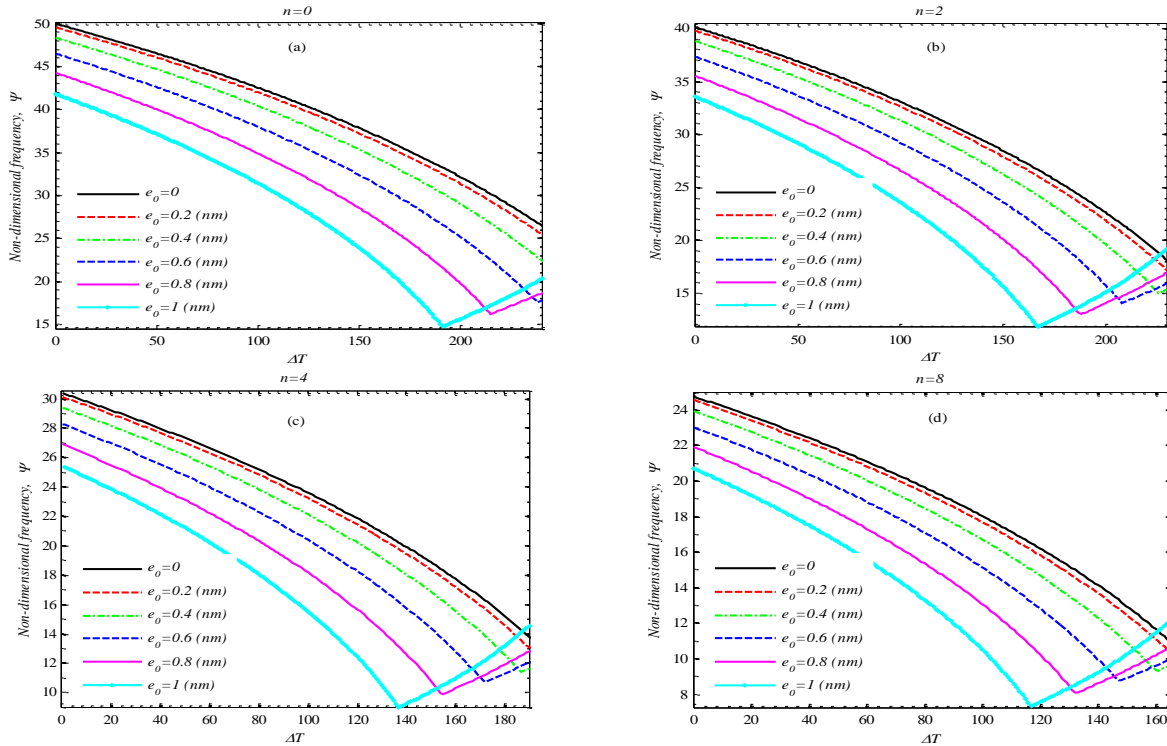


**Fig. 22** Variations of the second non-dimensional frequency of the propped cantilever FG nano-beam with respect to temperature change for different values of gradient indexes and nonlocal parameters  $h=2b/5=L/50=0.2$  ( $n$ ) and  $\Phi=0$ .

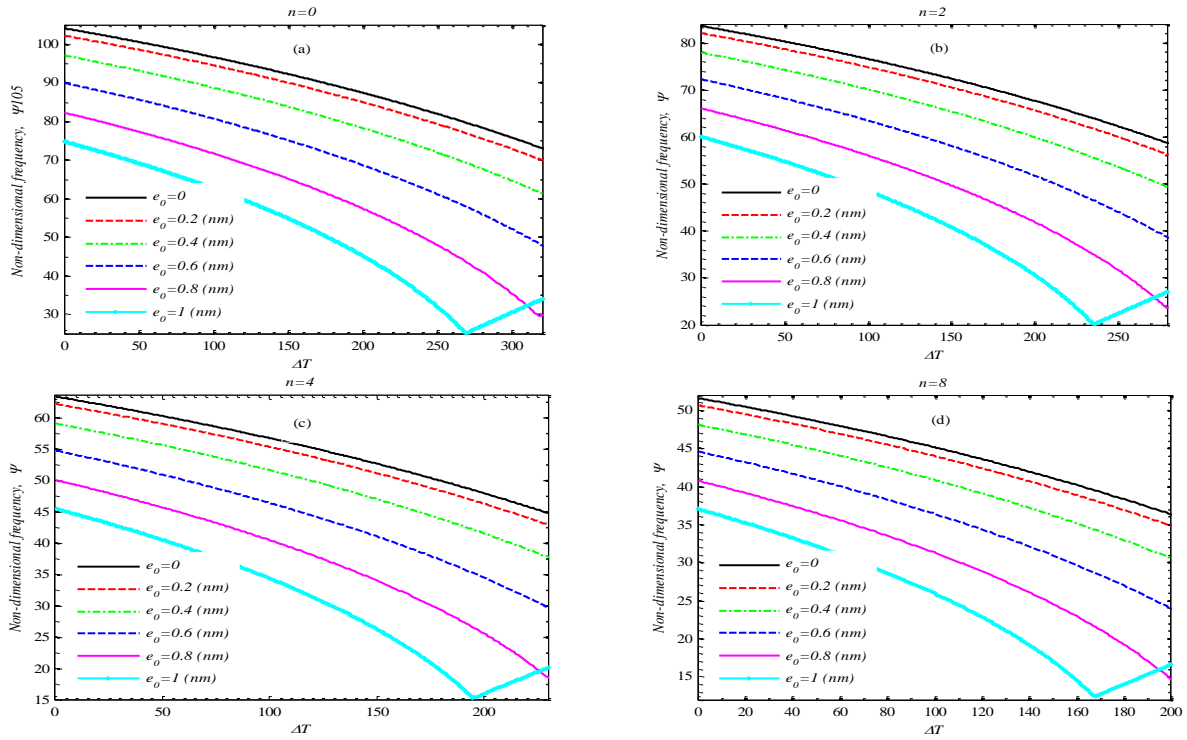


**Fig. 23** Variations of the third non-dimensional frequency of the propped cantilever FG nano-beam with respect to temperature change for different values of gradient indexes and nonlocal parameters,  $h=2b/5=L/50=0.2$  ( $n$ ) and  $\Phi=0$ .

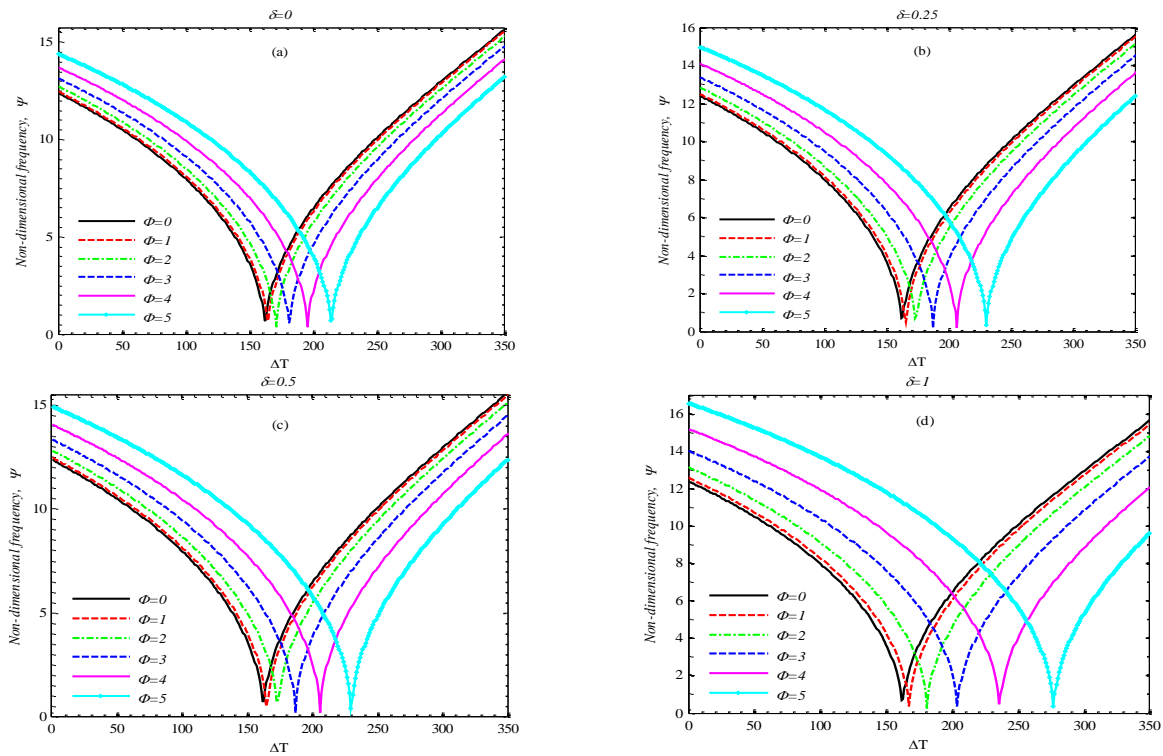


**Fig. 24** Variations of the fundamental non-dimensional frequency of the propped cantilever FG nano-beam with respect to temperature change for different values of hub radius and non-dimensional angular velocities,  $h=b/4=L/40=0.25$  ( $nm$ ) and  $n=0.2$ .

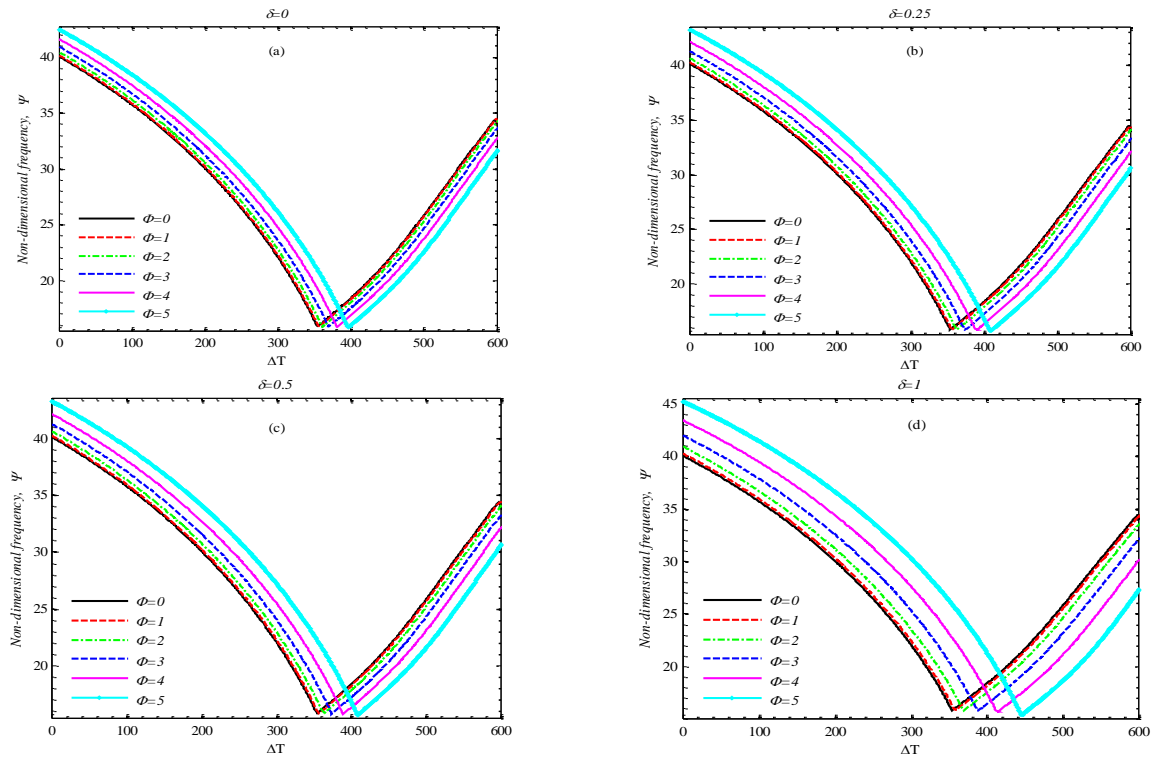


**Fig. 25** Variations of the second non-dimensional frequency of the propped cantilever FG nano-beam with respect to temperature change for different values of hub radius and non-dimensional angular velocities,  $h=b/4=L/40=0.25$  (nm) and  $n=0.2$ .

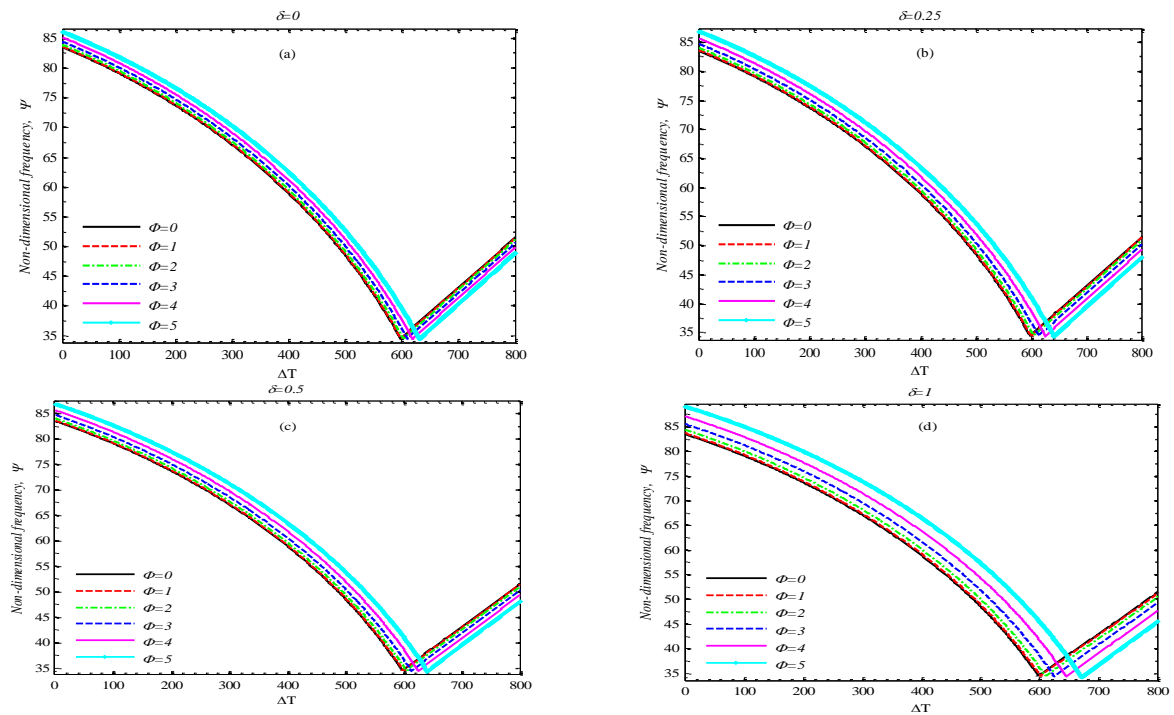


**Fig. 26** Variations of the third non-dimensional frequency of the propped cantilever FG nano-beam with respect to temperature change for different values of hub radius and non-dimensional angular velocities,  $h=b/4=L/40=0.25$  (nm) and  $n=0.2$ .

## 5 CONCLUSIONS

In this process the effect of the nonlocal small-scale, material property gradient index, hub radius of the first three vibrations of the temperature-dependent FG nano-beam s subjected to the non-linear temperature distribution with considering terms of rotating for two types of cantilever and propped cantilever are investigated. By means of GDQM. Eringen's theory of nonlocal elasticity with Euler-Bernoulli beam theory are employed to model the nano-beam. It is observed that, various parameters such as nonlocal parameter, gradient index, angular velocity, hub radius, temperature-dependent material properties and environment temperature have significantly influence on the vibrational frequencies of FG nano-beam s. It is obtained that, the non-dimensional frequencies increase with the rotating angular velocity for both cantilever and propped cantilever models. For angular velocity, the observed non-dimensional fundamental frequency increases with the nonlocal parameter for cantilever model. This trend is opposite for the propped cantilever where the nonlocal frequencies are lower than local ones but second and third modes of vibration of two models are similar. For nano-cantilever, the fundamental non-dimensional frequencies are being close to each other at low rotating velocities but for nano-propped cantilever, it occurs at high rotating velocities. It is observed that, for nano-cantilever, variation of fundamental frequency through temperature changes depend on nonlocal parameters. First three modes of propped cantilever frequency decrease with the increase in temperature and tend to the lowest value at the critical temperature. This decrease in frequency is because of reducing beam stiffness due to thermally caused compressive stress. However, after the critical temperature point, the frequencies increase with the growth of temperature. In addition, it is concluded that under non-linearly temperature increase, increase the FG index value leads to the decrease in frequency and with increasing gradient index, the branching point is created at lower temperature, because at the lower gradient indexes, the structure stiffness will be more is due to the lower gradient indexes the structure is more stiffness. Also, the moment rotating and inertia increase due to rising the hub radius, makes the frequency to increase.

## REFERENCES

- [1] Aranda-Ruiz J., Loya J., Fernandez-Saez J., 2012, Bending vibrations of rotating nonuniform nanocantilevers using the Eringen nonlocal elasticity theory, *Composite Structures* **94**: 2990-3001.
- [2] Bath J., Turberfield A. J., 2007, DNA nanomachines, *Nature Nanotechnology* **2**: 275-284.
- [3] Bellman R., Casti J., 1971, Differential quadrature and long-term integration, *Journal of Mathematical Analysis and Applications* **34**: 235-238.
- [4] Bellman R., Kashef B., Casti J., 1972, Differential quadrature: a technique for the rapid solution of nonlinear partial differential equations, *Journal of Computational Physics* **10**: 40-52.
- [5] Chen L., Nakamura M., Schindler T. D., Parker D., Bryant Z., 2012, Engineering controllable bidirectional molecular motors based on myosin, *Nature Nanotechnology* **7**: 252-256.
- [6] Civalek Ö., 2004, Application of differential quadrature (DQ) and harmonic differential quadrature (HDQ) for buckling analysis of thin isotropic plates and elastic columns, *Engineering Structures* **26**: 171-186.
- [7] Ebrahimi F., Barati M. R., 2017, Vibration analysis of viscoelastic inhomogeneous nano-beam s incorporating surface and thermal effects, *Applied Physics A* **123**: 5.
- [8] Ebrahimi F., Salari E., 2015, Thermo-mechanical vibration analysis of nonlocal temperature-dependent FG nano-beam s with various boundary conditions, *Composites Part B: Engineering*, **78**: 272-290.
- [9] Eringen A. C., 1983, On differential equations of nonlocal elasticity and solutions of screw dislocation and surface waves, *Journal of Applied Physics* **54**: 4703-4710.
- [10] Ghadiri M., Hosseini S., Shafiei N., 2015, A power series for vibration of a rotating nano-beam with considering thermal effect, *Mechanics of Advanced Materials and Structures* **2015**: 1-30.
- [11] Ghadiri M., Shafiei N., 2015, Nonlinear bending vibration of a rotating nano-beam based on nonlocal Eringen's theory using differential quadrature method, *Microsystem Technologies* **2015**: 1-15.
- [12] Ghadiri M., Shafiei N., Akbarshahi A., 2016, Influence of thermal and surface effects on vibration behavior of nonlocal rotating Timoshenko nano-beam, *Applied Physics A* **122**: 1-19.
- [13] Ghadiri M., Shafiei N., Safarpour H., 2017, Influence of surface effects on vibration behavior of a rotary functionally graded nano-beam based on Eringen's nonlocal elasticity, *Microsystem Technologies* **23**: 1045-1065.
- [14] Ghorbanpour-Arani A., Rastgoo A., Sharafi M., Kolahchi R., Arani A. G., 2016, Nonlocal viscoelasticity based vibration of double viscoelastic piezoelectric nano-beam systems, *Meccanica* **51**: 25-40.
- [15] Goel A., Vogel V., 2008, Harnessing biological motors to engineer systems for nanoscale transport and assembly, *Nature Nanotechnology* **3**: 465-475.
- [16] Hu B., Ding Y., Chen W., Kulkarni D., Shen Y., Tsukruk V. V., Wang Z. L., 2010, External-strain induced insulating phase transition in VO<sub>2</sub> nano-beam and its application as flexible strain sensor, *Advanced Materials* **22**: 5134-5139.

- [17] Lee L. K., Ginsburg M. A., Cravace C., Donahoe M., Stock D., 2010, Structure of the torque ring of the flagellar motor and the molecular basis for rotational switching, *Nature* **466**: 996-1000.
- [18] Lu P., Lee H., Lu C., Zhang P., 2006, Dynamic properties of flexural beams using a nonlocal elasticity model, *Journal of Applied Physics* **99**: 073510.
- [19] Lubbe A. S., Ruangsupapichat N., Caroli G., Feringa B. L., 2011, Control of rotor function in light-driven molecular motors, *The Journal of Organic Chemistry* **76**: 8599-8610.
- [20] Maraghi Z. K., Arani A. G., Kolahchi R., Amir S., Bagheri M., 2013, Nonlocal vibration and instability of embedded DWBNNT conveying viscose fluid, *Composites Part B: Engineering* **45**: 423-432.
- [21] Mindlin R. D., 1964, Micro-structure in linear elasticity, *Archive for Rational Mechanics and Analysis* **16**: 51-78.
- [22] Mirjavadi S. S., Rabby S., Shafiei N., Afshari B. M., Kazemi M., 2017, On size-dependent free vibration and thermal buckling of axially functionally graded nano-beam s in thermal environment, *Applied Physics A* **123**: 315.
- [23] Narendar S., 2012, Differential quadrature based nonlocal flapwise bending vibration analysis of rotating nanotube with consideration of transverse shear deformation and rotary inertia, *Applied Mathematics and Computation* **219**: 1232-1243.
- [24] Pradhan S., Murmu T., 2010, Application of nonlocal elasticity and DQM in the flapwise bending vibration of a rotating nanocantilever, *Physica E: Low-Dimensional Systems and Nanostructures* **42**: 1944-1949.
- [25] Rahmani O., Pedram O., 2014, Analysis and modeling the size effect on vibration of functionally graded nano-beam s based on nonlocal Timoshenko beam theory, *International Journal of Engineering Science* **77**: 55-70.
- [26] Shu C., 2000, *Differential Quadrature and Its Application in Engineering*, Springer.
- [27] Shu C., Richards B.E., 1992, Application of generalized differential quadrature to solve two-dimensional incompressible Navier-Stokes equations, *International Journal for Numerical Methods in Fluids* **15**: 791-798.
- [28] Tauchert T. R., 1974, *Energy Principles in Structural Mechanics*, McGraw-Hill Companies.
- [29] Thai H.T., 2012, A nonlocal beam theory for bending, buckling, and vibration of nano-beam s, *International Journal of Engineering Science* **52**: 56-64.
- [30] Tierney H. L., Murohy C. J., Jewell A. D., Baber A. E., Iski E. V., Khodaverdian H. Y., Mcguire A. F., Klebanov N., Sykes E. C. H., 2011, Experimental demonstration of a single-molecule electric motor, *Nature Nanotechnology* **6**: 625-629.
- [31] Toupin R. A., 1962, Elastic materials with couple-stresses, *Archive for Rational Mechanics and Analysis* **11**: 385-414.
- [32] Vandelden R. A., Terwiel M. K., Pollard M. M., Vicario J., Koumura N., Feringa B. L., 2005, Unidirectional molecular motor on a gold surface, *Nature* **437**: 1337-1340.
- [33] Wang C., Zhang Y., He X., 2007, Vibration of nonlocal Timoshenko beams, *Nanotechnology* **18**: 105401.
- [34] Xing Y., Liu B., 2009, High-accuracy differential quadrature finite element method and its application to free vibrations of thin plate with curvilinear domain, *International Journal for Numerical Methods in Engineering* **80**: 1718-1742.
- [35] Zhong H., Yue Z., 2012, Analysis of thin plates by the weak form quadrature element method, *Science China Physics, Mechanics and Astronomy* **55**: 861-871.